**Department of Energy**
**National Nuclear Security Administration**
Washington, DC 20585

JUN 27 2002

Mr. Herbert N. Berkow
Document Control Desk
U.S. Nuclear Regulatory Commission
Washington D.C. 20555

Proj 697
50-390/391

SUBJECT: Project Number 697 - Post-Irradiation Report for the Tritium-Producing Burnable Absorber Rods Irradiated in the Watts Bar Nuclear Plant

Dear Mr. Berkow:

This letter is in response to Section 3.9 (TPBAR Irradiation Tests and Test Data Summary) of the Safety Evaluation Report related to the Department of Energy's topical report on the tritium core (NUREG-1672) dated May 1999, which stated that the following:

> "Information from the LTA demonstration is expected to be provided to the NRC staff for their review prior to issuing a plant-specific license amendment for irradiation production of quantities of TPBARs. "

Attached is the final unclassified report on the LTA demonstration entitled "Postirradiation Examination Report for the Tritium-Producing Burnable Absorber Rods Irradiated in the Watts Bar Nuclear Plant (PNNL-13931)" dated June 2002. The classified details are available for review upon request.

If you have any questions, please call me at (202) 586-0838.

Sincerely,

Max J. Clausen
Director
Tritium Production
Office of Srategic Materials and Transportation

Enclosure

Printed with soy ink on recycled paper

D051

cc:
O. Taylor, NA-125 (w/o enclosure)
S. Stack, NA-125 (w/o enclosure)
J. Chardos, TVA, (w/o enclosure)
M. Travis, WesDyne (w/o enclosure)
C. Thornhill, PNNL (w/o enclosure)
G. Sorensen, PNNL (w/o enclosure)
NA-125 RMS/SS (CLWR/05-01)

PNNL-13931

Pacific Northwest
National Laboratory
Operated by Battelle for the
U.S. Department of Energy

# Postirradiation Examination Report for the Tritium-Producing Burnable Absorber Rods Irradiated in the Watts Bar Nuclear Plant

D. D. Lanning
D. L. Baldwin
M. E. Cunningham
S. C. Marschman

June 2002

Prepared for the U.S. Department of Energy
under Contract DE-AC06-76RL01830

**EXPORT CONTROLLED INFORMATION**
Contains technical data whose export is restricted by statute 15 CFR 730-774. Violations may result in administrative, civil, or criminal penalties. Limited dissemination to U.S. Department of Energy and major U.S. DOE contractors. The cognizant program manager must approve other dissemination. This notice shall not be separated from the attached document.
Reviewer Darlene Varley Date 5/29/2002

**DISCLAIMER**

This report was prepared as an account of work sponsored by an agency of the United States Government. Neither the United States Government nor any agency thereof, nor Battelle Memorial Institute, nor any of their employees, makes **any warranty, express or implied, or assumes any legal liability or responsibility for the accuracy, completeness, or usefulness of any information, apparatus, product, or process disclosed, or represents that its use would not infringe privately owned rights.** Reference herein to any specific commercial product, process, or service by trade name, trademark, manufacturer, or otherwise does not necessarily constitute or imply its endorsement, recommendation, or favoring by the United States Government or any agency thereof, or Battelle Memorial Institute. The views and opinions of authors expressed herein do not necessarily state or reflect those of the United States Government or any agency thereof.

PACIFIC NORTHWEST NATIONAL LABORATORY
*operated by*
BATTELLE
*for the*
UNITED STATES DEPARTMENT OF ENERGY
*under Contract DE-AC06-76RL01830*

This document was printed on recycled paper.
(8/00)

PNNL-13931

# Postirradiation Examination Report for the Tritium-Producing Burnable Absorber Rods Irradiated in the Watts Bar Nuclear Plant

D.D. Lanning
D.L. Baldwin
M.E. Cunningham
S.C. Marschman

June 2002

Prepared for
the U.S. Department of Energy
under Contract DE-AC06-76RL01830
Pacific Northwest National Laboratory
Richland, Washington 99352

**EXPORT CONTROLLED INFORMATION**
Contains technical data whose export is restricted by statute 15 CFR 730-774. Violations may result in administrative, civil, or criminal penalties. Limited dissemination to U.S. Department of Energy and major U.S. DOE contractors. The cognizant program manager must approve other dissemination. This notice shall not be separated from the attached document.
Reviewer Darlene Varley Date 5/29/2002

# Summary

The *Tritium Production Core (TPC) Topical Report (unclassified, non- proprietary version)* (Westinghouse 1999) identified steps to be taken by the U.S. Department of Energy, Tennessee Valley Authority (TVA), and Pacific Northwest National Laboratory (PNNL) to monitor and evaluate performance of 32 tritium-producing burnable absorber rods (TPBARs) during and after their irradiation in four lead test assemblies (LTAs) in cycle 2 of the Watts Bar Nuclear Power Plant (WBN). This report documents the monitoring and evaluation that was performed.

As part of a Department of Energy project, a confirmatory demonstration of the performance of TPBARs, TVA contracted to irradiate four LTAs for one reactor operating cycle in the WBN. Thirty-two TPBARs were fabricated by PNNL in the summer of 1997 and shipped to the Westinghouse Fuel Fabrication Facility in Columbia, South Carolina, where four LTAs, each with eight TPBARs, were assembled and then shipped to WBN for irradiation. The U.S. Nuclear Regulatory Commission issued a license amendment on September 15, 1997, authorizing WBN to irradiate the four LTAs for one operating cycle. The LTAs were placed in the WBN core on September 25, 1997. WBN achieved full power on October 17, 1997, and operated with the LTAs until February 27, 1999. The LTAs were removed from the WBN core on March 8, 1999, and from their host fuel assemblies on March 19, 1999, when they were placed in transportation arrays in the WBN spent fuel pool. From July to September 1999, the LTAs were individually shipped from WBN to Argonne National Laboratory-West (ANL-W), located on the Idaho National Engineering and Environmental Laboratory site near Idaho Falls, Idaho. Nondestructive postirradiation examinations were conducted on all 32 TPBARs at ANL-W. Four TPBARs were then shipped in December 2000 from ANL-W to PNNL for destructive postirradiation examination.

**Overview**

Based on monitoring performed during the 17-month irradiation in WBN and the subsequent postirradiation examinations, the TPBARs performed as expected during irradiation. WBN experienced no difficulties during the cycle attributable to the LTAs. Evaluation of the tritium concentrations in the reactor coolant determined that the LTA irradiation met its design goal of releasing less than 6.7 Ci per TPBAR per year. Following irradiation and shipping for nondestructive postirradiation examination, the TPBARs were intact and undamaged. The nondestructive and destructive postirradiation examinations confirmed that the TPBARs performed as expected.

Postirradiation visual examination of the TPBARs in the WBN spent fuel pool showed no visible indications of damage to the rods or unusual amounts of corrosion. The TPBARs were easily removed from their host fuel assemblies and reinserted into shipping arrays, thus indicating no unusual growth, bow, or other physical distortion as a result of irradiation.

Nondestructive postirradiation examinations at ANL-W confirmed that the cladding of all 32 TPBARs remained intact during irradiation and postirradiation handling and shipping. Neutron radiography and full-length axial spectral gamma scanning confirmed the physical integrity of internal components. Analysis of measured rod gas pressures, void volumes, and gas composition confirmed that

the TPBAR internal components functioned as designed; that is, the tritium production was as expected and the tritium was contained in the internal components.

Destructive postirradiation examinations were conducted at PNNL on four of the TPBARs. These examinations included measuring lithium isotopic ratios to determine lithium burnup and tritium production, performing tritium assays to evaluate the quantity and distribution of tritium within the TPBARs, performing hydrogen assays to evaluate the pickup of hydrogen from the reactor coolant, performing postirradiation measurements of the performance of the getters, and performing optical metallography of the components to observe visual changes in the TPBAR components. The results of the destructive examinations confirmed that the TPBARs performed as expected and that no changes are required to the current TPBAR design.

In summary, the irradiation was completed without any adverse impacts on reactor operation or on the TPBARs, and all LTA expectations were met. All results were as expected, and no changes to the TPBAR design are necessary as a result of the postirradiation examination data.

**Performance During Irradiation and Storage**

During the period of time the TPBARs were resident in the WBN core, TVA performed weekly monitoring of the reactor coolant for tritium concentration. Evaluation of the measured tritium concentrations in the reactor coolant determined that the LTA TPBARs met their design goal of releasing less than 6.7 Ci per TPBAR per year.

In preparation for shutdown of WBN from cycle 2, PNNL requested that TVA take samples of the spent fuel pool water and measure tritium concentration levels prior to placing the LTAs in the spent fuel pool. This monitoring began 2 weeks before shutdown, with samples taken on a daily basis prior to placing the TPBARs in the spent fuel pool. Monitoring of the spent fuel pool continued on a weekly basis for the entire time the TPBARs were in the spent fuel pool (March to September 1999). Monitoring showed no increase in tritium in the spent fuel pool prior to discharge and no change during the time the TPBARs were stored.

**Nondestructive Postirradiation Examinations**

Nondestructive postirradiation examinations of the irradiated TPBARs were performed by ANL-W beginning in September 1999 and were completed in June 2000. The following nondestructive examinations were performed on all 32 TPBARs at ANL-W.

- Visual examination and photography – All TPBARs were examined visually over their full length in at least two orthogonal orientations. Handling scratches, variations in the oxide appearance, and small amounts of reactor coolant system "crud" deposit were observed. No damage to the cladding was observed.

- Rod length, diameter, and bow measurement – Postirradiation diameters were approximately the same as pre-irradiation; TPBAR lengths increased approximately 0.1 inch during the irradiation, which was less than allowed in the design; and maximum TPBAR bow was less than 0.5 inch.

- Axial gamma scanning – Axial profiles of activation products in the TPBARs confirmed the axial power profile for the irradiation. Uniform gamma activities among the TPBARs confirmed the relatively flat distribution of power across the LTAs.

- Neutron radiography – All rods were neutron radiographed over their entire length. These radiographs provided a good "picture" of the axial location and physical state of the pencils and the absorber pellet columns. The radiographs confirmed that the internal components maintained their physical integrity during irradiation and postirradiation shipping and handling. Cracked absorber pellets were observed, but they were maintained in position by the getter and liner. No opening of axial gaps between pencils or between pellets was observed.

- Rod puncture – All TPBARs were punctured, void volume and gas pressure were measured, and gas composition was measured. Analysis of the void volumes, gas pressures, and gas compositions confirmed the predicted tritium production; that is, tritium production derived from these data agreed with the predicted tritium production. Analysis of the gas composition also confirmed that the internal components performed their function of retaining the tritium.

**Destructive Postirradiation Examinations**

Four TPBARs were cut into three segments each by ANL-W and then shipped to PNNL in December 2000. The destructive examinations were performed by PNNL beginning in January 2001 and completed in March 2002. One TPBAR was extensively examined along its full length while confirmatory measurements were made on the other three TPBARs. The following destructive examinations were performed on the four TPBARs at PNNL:

- Assay for lithium isotopic ratio – The results were used to evaluate lithium burnup and tritium production and confirmed the expected tritium production derived from the analysis of TPBAR void volumes, gas pressures, and gas compositions.

- Assay for tritium concentrations in the getters, pellets, and liners – The results were used to evaluate the distribution of tritium in the internal TPBAR components and confirmed the retention of the tritium in the TPBAR components.

- Assay for hydrogen concentrations in the getters and liners – The results were used to evaluate the ingress of hydrogen from the reactor coolant and confirmed that hydrogen pickup by the TPBARs was below the upper bound set by the design.

- Assay for helium concentration in the pellets – The results were used to refine the tritium production calculations.

- Measurement of the hydrogen pickup rate of irradiated getters – The results confirmed that the end-of-irradiation performance of the getters met the design requirements.

- Optical metallography and scanning electron microscopy – The results confirmed that no unexpected microstructural changes occurred during the irradiation.

The results from the destructive postirradiation examinations were as expected and showed that the performance of all four examined TPBARs was consistent.

Evaluation of the nondestructive and destructive postirradiation examination data shows that the performance of the TPBARs met the design goals and assumptions. No changes to the current TPBAR design are indicated from the postirradiation examination data.

# Acknowledgements

Many persons who are not listed as authors, reviewers, or references have contributed to the irradiation, shipping, and postirradiation examinations of the lead test assembly tritium-producing burnable absorber rods. Recognizing that we cannot acknowledge everyone, and taking the risk that we have inadvertently omitted someone who should be recognized, we gratefully acknowledge the contributions of these major contributors:

| **Argonne National Laboratory-West Staff** | |
|---|---|
| David Duncan | Richard Wisner |
| all the technical staff of the Hot Fuels Examination Facility | |
| **Columbia Fuel Fabrication Facility** | |
| Phil Stroud | Doug Trevett |
| **Pacific Northwest National Laboratory Staff** | |
| (Radiochemical Processing Laboratory) | |
| Pam Berry | Bob Orton |
| Stan Bos | David Ortiz |
| Steve Halstead | Tim Reining |
| Paul MacFarlan | Mike Urie |
| Jim Matheson | Dennis Wester |
| Clay O'Laughlin | |
| (TTQP and Other Staff) | |
| Cheryl Thornhill | Bruce Reid |
| Una Carriera | Ron Schrotke |
| Glenn Hollenberg | Gary Sevigny |
| Kate Larson | Gerald Sorensen |
| Ed Love | |
| **Tennessee Valley Authority Staff** | |
| Richard Boren | Craig Faulkner |
| Jim Chardos | |
| **U.S. Department of Energy Staff** | |
| Stephen Sohinki | Max Clausen |
| Mike Klimas | O. Wesley Taylor |
| Lewis Steinhoff | |

Many other persons not listed also assisted with the irradiation, shipping, and postirradiation examinations of the LTA. For all their help, we are extremely grateful.

# Acronyms and Abbreviations

| Term | Definition |
|---|---|
| ANL-W | Argonne National Laboratory-West |
| Ar | argon |
| ATR | Advanced Test Reactor |
| cc | cubic centimeter |
| CFFF | Columbia Fuel Fabrication Facility |
| Ci | curie |
| Cl | chlorine |
| Co | cobalt |
| DE | destructive examination |
| EOL | end of life |
| F | fluorine |
| g | gram |
| GASR | Gas Analysis, Sample, and Recharge (system) |
| H | hydrogen |
| He | helium |
| HLRF | High Level Radiation Facility |
| ID | inside diameter |
| Li | lithium |
| $LiAlO_2$ | lithium aluminate |
| LTA | lead test assembly |
| mg | milligram |
| mm | millimeter |
| N | nitrogen |
| Nb | niobium |
| NDE | nondestructive examination |
| NIST | National Institute of Standards and Technology |

| Term | Definition |
|---|---|
| OD | outside diameter |
| PIE | postirradiation examination |
| PNNL | Pacific Northwest National Laboratory |
| psia | pounds per square inch absolute |
| STP | standard temperature and pressure |
| T | tritium |
| THO | tritiated water |
| TPBAR | tritium-producing burnable absorber rod |
| TPC | Tritium Production Core (topical report) |
| TTQP | Tritium Target Qualification Project |
| TVA | Tennessee Valley Authority |
| WBN | Watts Bar Nuclear (power plant) |
| Zr | zirconium |
| μm | micrometer |

# Contents

Summary ..... iii

Acknowledgements ..... vii

Acronyms and Abbreviations ..... ix

1.0 Introduction ..... 1

1.1 TPBAR Design ..... 3

1.2 TPBAR Irradiation in WBN ..... 5

2.0 Nondestructive Examinations ..... 9

2.1 Disassembly of the LTAs ..... 9

2.2 Visual Examination of the TPBARs ..... 12

2.3 Neutron Radiography ..... 21

2.4 Axial Gamma Scanning ..... 22

2.5 Metrology ..... 23

2.5.1 TPBAR Diameter ..... 23

2.5.2 TPBAR Length and Bow ..... 26

2.6 Rod Puncture and Gas Analysis ..... 30

2.6.1 Rod Puncture, Void Volume, Gas Pressure ..... 30

2.6.2 Gas Composition Analysis ..... 30

2.7 Other Examinations Performed by ANL-W ..... 31

2.8 Evaluations of the Nondestructive Data ..... 32

2.8.1 Predicted Versus Measured Tritium/Helium Production ..... 32

2.8.2 Pencil and Liner Length Change from Neutron Radiography ..... 35

3.0 Destructive Examinations ..... 37

3.1 TPBAR Segmenting for Shipment to PNNL ..... 37

3.2 Summary of the Sectioning and Examination Plan ..... 37
3.3 Rod Sectioning, Component Separation, and Data Analysis Approach ..... 38
3.3.1 Pellet Lithium Isotopic Analyses and Lithium Burnup Estimates ..... 39
3.3.2 Tritium Recovery, Concentration, and Loading ..... 40
3.3.3 Protium Concentration and Loading ..... 40
3.3.4 Pellet He-4 Recovery ..... 41
3.4 Assay Results for Individual TPBARs ..... 41
3.4.1 Assay Results for T0291 ..... 41
3.4.2 Assay Results for T0281 ..... 43
3.4.3 Assay Results for T0166 ..... 44
3.4.4 Assay Results for T0195 ..... 45
3.5 Discussion of Li-6 Burnup Results ..... 45
3.5.1 Total He-4 Production and Derived Li-6 Burnup ..... 45
3.5.2 Li-6 Burnup from Isotopic Data Compared to Derived Burnup ..... 46
3.6 Evaluation of Tritium and Protium Assay and Getter Rate Results ..... 49
4.0 Optical Metallography ..... 51
4.1 Sample Cutting ..... 51
4.2 Sample Mounting ..... 51
4.3 Sample Grinding ..... 51
4.4 Sample Etching ..... 52
4.5 Optical Examination ..... 52
4.6 Examination Results ..... 53
5.0 Conclusions ..... 55
6.0 References ..... 57

# Figures

Figure 1. Isometric Section of a TPBAR ..... 4

Figure 2. WBN Power History during Cycle 2 ..... 6

Figure 3. Schematic of LTA/TPBAR Orientation in the WBN Core during Cycle 2 ..... 7

Figure 4. LTA 8TR004 in Disassembly Jig (Photo DD12224e) ..... 11

Figure 5. 18-Inch Region on TPBAR T0263 as Observed during LTA Disassembly (Photo T0263#1.8) ..... 12

Figure 6. Example of Handling Scratches, TPBAR T0256 (Photo 2560#2) ..... 14

Figure 7. Example of Cyclical/Helical Oxide Appearance, TPBAR T0256 (Photo 2560#8) ..... 15

Figure 8. Example of Light Gray Oxide Bands at Top of TPBAR T0238 (Photo 2380#1) ..... 16

Figure 9. 18-Inch Region on TPBAR T0238 ..... 17

Figure 10. Examples of End Plug Weld Condition at End of Irradiation ..... 18

Figure 11. Example of Circular Mark on TPBAR T0256 (Photo VEM 256#24) ..... 19

Figure 12. Photographs of Circumferential Scratch on TPBAR T0256 at 37 Inches ..... 20

Figure 13. Diameter Plot for TPBAR T0291, 0° ..... 24

Figure 14. Summary of TPBAR Length Measurements with Comparison to Pre-Irradiation Specification ..... 28

Figure 15. Summary of TPBAR Maximum Bow Values ..... 29

Figure 16. Example of TPBAR Bow ..... 29

Figure 17. Derived Tritium Production (from TPBAR Puncture Measurements) Compared to Predicted Production ..... 34

Figure 18. Comparison of He-3/He-4 Ratios to Estimated Tritium Production ..... 34

Figure 19. Comparison of Specified Pre-Irradiation Liner Length to Postirradiation Length Estimates for TPBAR T0166 ..... 36

Figure 20. Comparison of Specified Pre-Irradiation Liner Length to Postirradiation Length Estimates for TPBAR T0195 ..... 36

Figure 21. Measured and Derived Li-6 Burnup for TPBAR T0291 ..... 47

Figure 22. Measured and Derived Li-6 Burnup for TPBAR T0281 ..... 48

Figure 23. Measured and Derived Li-6 Burnup for TPBAR T0166 ..... 48

Figure 24. Measured and Derived Li-6 Burnup for TPBAR T0195 ..... 49

# Tables

Table 1. Nondestructive Examinations ..... 2

Table 2. Destructive Examinations ..... 3

Table 3. Selected LTA TPBAR Nominal Design Parameters ..... 4

Table 4. Summary of Average Postirradiation Diameter for the TPBARs ..... 25

Table 5. Summary of TPBAR Length and Bow Measurements ..... 27

Table 6. Derived and Predicted Tritium Production in LTA TPBARs ..... 33

Table 7. Lithium Isotopic Results and Lithium Burnup Estimates for T0291 ..... 42

Table 8. He-4 Recovery Data on Pellets from TPBAR T0291 ..... 43

Table 9. Lithium Isotopic Results and Lithium Burnup Estimates for T0281 ..... 43

Table 10. He-4 Recovery Data on Pellets from TPBAR T0281 ..... 44

Table 11. Lithium Isotopic Results and Lithium Burnup Estimates for T0166 ..... 44

Table 12. He-4 Recovery Data on Pellets from TPBAR T0166 ..... 44

Table 13. Lithium Isotopic Results and Lithium Burnup Estimates for T0195 ..... 45

Table 14. He-4 Recovery Data on Pellets from TPBAR T0195 ..... 45

# 1.0 Introduction

The Tritium Target Qualification Project (TTQP) at the Pacific Northwest National Laboratory (PNNL) supports the U.S. Department of Energy's Tritium Production Project to demonstrate and qualify the fabricability and viability of the getter-barrier design concept for tritium-producing burnable absorber rods (TPBARs) irradiated in a light-water reactor.

Thirty-two TPBARs were fabricated by PNNL in July 1997 for irradiation in four lead test assemblies (LTAs), each containing eight TPBARs. The U.S. Nuclear Regulatory Commission issued a license amendment on September 15, 1997, authorizing the Tennessee Valley Authority's Watts Bar Nuclear (WBN) Power Plant to irradiate the four LTAs for one operating cycle. The four LTAs were attached to baseplates at Westinghouse's Columbia Fuel Fabrication Facility (CFFF), inserted into host fuel assemblies, and then shipped to WBN for irradiation in cycle 2. After the irradiation, the LTAs and their host fuel assemblies were removed from the core and placed in the spent fuel pool. The LTAs were then transferred to transportation arrays and shipped to Argonne National Laboratory-West (ANL-W)at the Idaho National Engineering and Environmental Laboratory site near Idaho Falls, Idaho. At ANL-W, the LTAs were unloaded into the Hot Fuels Examination Facility and disassembled into the 32 individual TPBARs; then the 32 TPBARs were nondestructively examined. Four TPBARs were segmented by ANL-W into three pieces each for shipment to PNNL for destructive examination.

Test plans and specific requirements for the nondestructive and destructive postirradiation examination (PIE) of the LTA TPBARs were defined in several documents.[1] Table 1 and Table 2 list the required examinations, results to be obtained, and testing requirements to be met.

Two classified reports present the complete results of the postirradiation examinations. The nondestructive examination (NDE) data collected by ANL-W are reported in detail in the classified report, PNNL-TTQP-3-528, *Evaluation Report on Nondestructive Examination of LTA TPBARs* (U) (Lanning and Cunningham 2001). A review of the NDE data combined with a complete compilation of the destructive examination (DE) data and analyses and interpretation of all the PIE data are presented in the classified report, PNNL-TTQP-3-542, *Results of Nondestructive and Destructive Examinations on the LTA TPBARs* (U) (Lanning et al. 2002).

This unclassified report describes the NDE and DE methodology, presents unclassified excerpts of the NDE and DE data, summarizes the data analyses, and presents unclassified conclusions based on all PIE results. The remainder of this section of the report describes the fabrication and irradiation of the LTA TPBARs. Section 2.0 describes the NDE methodology and presents the NDE data. Section 3.0 describes the methodology and analysis of the DE data and presents unclassified excerpts of assay data. A description of the optical metallography is presented in Section 4.0. Conclusions are presented in Section 5.0.

---

[1] Classified documents that identify requirements for the nondestructive and destructive PIE are PNNL-TTQP-3-511, *Test Plan for Postirradiation Examination of LTA TPBARs* (U) (Lanning 2000a); PNNL-TTQP-3-509, *Technical Requirements Document for the Nondestructive Examination of the LTA TPBARs by ANL-W* (U) (Lanning 2000b);

**Table 1.** Nondestructive Examinations

| Examination | Results | Testing Requirement Addressed |
|---|---|---|
| Visual Examination | General condition, surface anomalies | Verification of no bulk boiling and of TPBAR surface condition |
| Neutron Radiography | Nondestructive view of rod internal components | Physical stability of components, especially pellets<br>Size of axial gaps<br>Presence or absence of liquid water |
| Rod Metrology | Length, diameter, deviation from straightness | Dimensional stability of TPBARs<br>Deviations from as-fabricated dimensions |
| Axial Gamma Scanning | Axial profiles of activation products | Relative exposure among TPBARs<br>Location of major axial gaps and interfaces |
| TPBAR Puncture and Gas Analyses | Plenum gas composition, TPBAR void volume, and gas pressure at time of puncture | TPBAR integrity<br>Tritium activity<br>TPBAR total tritium/helium production |

PNNL-TTQP-3-527, *Sectioning and Examination Plan for the LTA TPBARs* (U) (Lanning 2000c); PNNL-TTQP-1-686, *Information Requirements for Postirradiation Testing of the LTA TPBARs* (U) (Lanning and Gilbert 1998).

**Table 2.** Destructive Examinations

| Examination | Results | Testing Requirement Addressed | Components Involved |
|---|---|---|---|
| Lithium Isotopics | Section-average lithium isotopic distribution | Lithium burnup and local tritium production | Pellets |
| Tritium Assay | Tritium concentration | Tritium partition, distribution<br>Getter loading<br>Liner loading | Pellets<br>Getters<br>Liners<br>Disks* |
| Helium Assay | He-4 concentration | Residual helium | Pellets |
| Protium Assay | Protium concentration (and tritium concentration in metal components) | Protium distribution; estimate of protium ingress | Getters<br>Liners |
| Getter Rate Testing | End-of-life getter rate at standardized test conditions | Getter rate on irradiated getters | Getters |
| Optical Metallography and Scanning Electron Microscopy | Visual appearance of component materials at high magnification | Cladding permeation barrier condition<br>Getter plating condition and hydriding<br>Pellet microstructure and damage from irradiation<br>Liner oxidation<br>Weld integrity and crevice deposits | Cladding<br>End Plug Weld<br>Getters<br>Liners<br>Pellets |

* Not included in the current TPBAR design.

## 1.1 TPBAR Design

Selected nominal design parameters for the LTA TPBARs are listed in Table 3. An isometric illustration of the TPBAR is shown in Figure 1. The getter-barrier TPBAR design features sintered, high-density, annular, lithium aluminate pellets as the tritium-producing material, contained in special stainless-steel cladding tubes with aluminized barrier layers to inhibit hydrogen ingress and tritium permeation leakage. Special nickel-plated Zircaloy getter tubes are placed between the pellets and the cladding to capture tritium released from the pellets, and Zircaloy liner tubes run along the inner bore of the annular pellets to chemically reduce tritiated water (THO) vapor released from the pellets. The liner tubes also contain the pellets mechanically.

**Table 3.** Selected LTA TPBAR Nominal Design Parameters

| Parameter | Value* |
|---|---|
| TPBAR Overall Length (inch) | 152.37 +0.050 –0.210 |
| TPBAR Length, upper end plug shoulder to tip of lower end plug (inch) | 151.70 +0.050 –0.210 |
| Radial Dimensions (inch) | |
| Cladding Outside Diameter (OD) x Inside Diameter (ID), Uncoated | 0.381 x 0.336 |
| Pellet OD x ID | 0.303 x 0.223 |
| Liner OD x ID | 0.208 x 0.200 |
| Pencil Column Length (inch) | 142 (12 pencils) |
| He Fill Gas Pressure (atm absolute) | 1 |
| Li-6 Enrichment (atom %) | 21.3 |
| $LiAlO_2$ Density (% theoretical density) | 95 |

* PNNL-TTQP-1-1024, *TPBAR Design Drawings* (U) (Hagerty and Gates 1996)

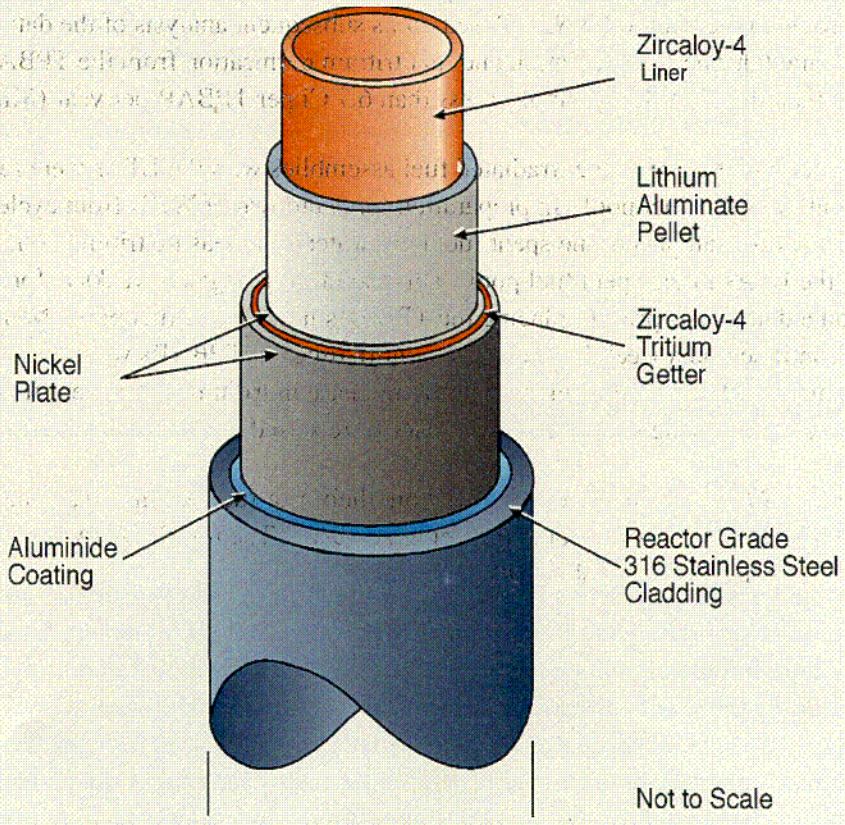


**Figure 1.** Isometric Section of a TPBAR



C01

## 1.2 TPBAR Irradiation in WBN

The TPBARs were shipped from PNNL on July 23, 1997, to the CFFF in Columbia, South Carolina. At this facility, eight TPBARs and 16 thimble plugs were attached to each of four hold-down plates to form four LTAs. The LTAs were then inserted into four host fuel assemblies that were placed in Westinghouse fuel shipping casks and shipped on July 29, 1997, from Columbia to the WBN plant in Spring City, Tennessee.

The fuel assemblies with the LTAs were loaded into the WBN core on September 27, 1997, and irradiated in cycle 2 for 471 effective full-power days from October 8, 1997, to February 27, 1999.

Figure 2 shows a plot of the WBN power history during cycle 2. Figure 3 is a schematic showing the relative orientations of the TPBARs in the LTAs and of the LTAs in the WBN core, and a correlation with Westinghouse's calculation of tritium production. This correlation is important in comparing predicted and measured tritium production and lithium burnup. The symmetrical placement of the LTAs around the center of the WBN core, and the predicted, nearly flat power distributions across the LTAs, indicate that there should be only about a 5% variation among the TPBARs.

During the irradiation of the LTAs, WBN regularly analyzed the reactor coolant for the concentration of tritium and provided the data to PNNL. Based on its subsequent analysis of the data, PNNL concluded that no TPBAR failed during the irradiation and that tritium permeation from the TPBARs into the reactor coolant was less than the LTA design limit of less than 6.7 Ci per TPBAR per year (Migliore 2000).

After the shutdown of cycle 2, the irradiated fuel assemblies with the LTAs were removed from the core and placed in the spent fuel pool. In preparation for shutdown of WBN from cycle 2, PNNL had requested that TVA take samples of the spent fuel pool water and measure tritium concentration levels prior to placing the LTAs in the spent fuel pool. This monitoring began 2 weeks before shutdown, with samples taken on a daily basis prior to placing the TPBARs in the spent fuel pool. Monitoring of the spent fuel pool continued on a weekly basis for the entire time the TPBARs were in the spent fuel pool (March to September 1999). Monitoring showed no increase in tritium in the spent fuel pool prior to discharge and no change during the time the TPBARs were stored.

On March 19, 1999, the LTAs were removed from their host fuel assemblies, visually inspected, and then placed into transportation arrays for shipment to ANL-W. The four LTAs were shipped individually to ANL-W from July through September 1999.

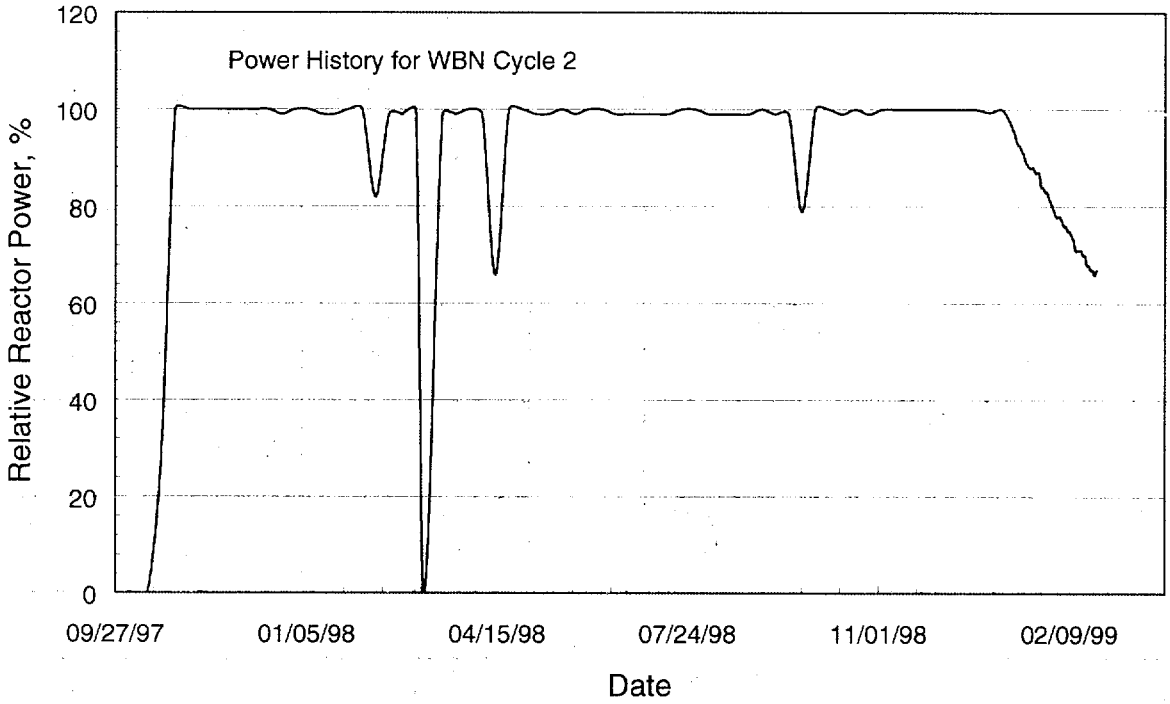


**Figure 2.** WBN Power History during Cycle 2

| LTA 8TR003<br>Shipped to CFFF in Container TP04<br>Irradiated in Fuel Assembly D55 | | | | | | LTA 8TR001<br>Shipped to CFFF in Container TP02<br>Irradiated in Fuel Assembly D53 | | | | |
|---|---|---|---|---|---|---|---|---|---|---|
| T0277<br>MO18<br>E | | | | T0290<br>MO20<br>C | | ***T0291***<br>***MO10***<br>***G*** | | | | T0169<br>MO12<br>E |
| | | T0183<br>MO19<br>D | | | | | | T0168<br>MO11<br>F | | |
| | T0210<br>MO25<br>F | | T0260<br>MO21<br>B | | | | ***T0281***<br>***MO17***<br>***H*** | | T0237<br>MO13<br>D | |
| | | T0262<br>MO23<br>H | | | | | | T0238<br>MO15<br>B | | |
| T0225<br>MO24<br>G | | | | T0217<br>MO22<br>A | | T0171<br>MO16<br>A | | | | T0256<br>MO14<br>C |
| | | | | | CL | | | | | |
| T0215<br>MO26<br>C | | | | T0241<br>MO28<br>A | | ***T0195***<br>***MO02***<br>***A*** | | | | T0209<br>MO04<br>G |
| | | T0202<br>MO27<br>B | | | | | | T0207<br>MO03<br>H | | |
| | T0266<br>MO33<br>D | | T0165<br>MO29<br>H | | | | T0205<br>MO09<br>B | | T0263<br>MO05<br>F | |
| | | T0176<br>MO33<br>F | | | | | | T0261<br>MO07<br>D | | |
| T0287<br>MO32<br>E | | | | T0232<br>MO30<br>G | | T0206<br>MO08<br>C | | | | ***T0166***<br>***MO06***<br>***E*** |
| LTA 8TR002<br>Shipped to CFFF in Container TP03<br>Irradiated in Fuel Assembly D54 | | | | | | LTA 8TR004<br>Shipped to CFFF in Container TP01<br>Irradiated in Fuel Assembly D56 | | | | |

Key: T0xxx = number assigned to TPBAR by TTQP
MOxx = number assigned to TPBAR by Westinghouse for tracking purposes during LTA assembly
i = letter corresponding to assembly position in Westinghouse's production calculations; the ▯A▯ position is always toward the core centerline.

The ▯Y▯ corner of the fuel assemblies is always toward the northwest, which is the upper left in this schematic. The four TPBARs identified by italics and bold (for example, ***T0291***) were selected for DE at PNNL.

**Figure 3.** Schematic of LTA/TPBAR Orientation in the WBN Core during Cycle 2

# 2.0 Nondestructive Examinations

Activities at ANL-W consisted of unloading the LTAs in the transportation arrays from the NAC International legal-weight truck cask, removing the TPBARs from the LTA hold-down plates, and then performing the examinations specified by PNNL (Lanning 2000b).

The examinations conducted on the TPBARs consisted of neutron radiography; visual examination; metrology (diameter, length, and bow); spectral axial gamma scanning; and rod puncture to measure internal gas pressure, gas composition, and rod internal volume.

Data were transferred from ANL-W to PNNL in discrete transmittal packages. Selected results are provided in this report to illustrate specific observations and/or features; see Lanning and Cunningham (2001) for a complete description of the NDE results. All neutron radiographs, photographs, and the digital data from these examinations are stored in PNNL records with the data transmittals.

One factor that complicated the TPBAR examinations at ANL-W was the length of the TPBARs (~153 inches). The examination stations in the Hot Fuels Examination Facility at ANL-W were built for shorter rods. To accommodate the long lengths, three approaches were needed.

- For the neutron radiography, it was necessary to invert the TPBARs to radiograph the upper portion of the TPBARs. The lower ~100 inches of the TPBARs were radiographed first, then the TPBARs were inverted and the upper ~60 inches of the TPBARs were radiographed.

- For the metrology, full-length axial gamma scanning, and detailed visual examination, the support stages were modified. The upper portions of the TPBARs (except for approximately the top 10 inches) were examined or measured; then the support stage was lifted so that the lower portions of the TPBARs could be examined or measured. Pits in the hot cell floor were of sufficient depth to accommodate the length of the TPBARs.

- For the rod puncture, it was necessary to lower the TPBARs fully to the bottom of the pit so that the laser beam would be aimed at a section of the plenum above the upper getter disk. During this period, the TPBARs were self supporting and were clamped into the puncture rig. An informal evaluation by PNNL was performed to ensure that the TPBARs could support themselves in this orientation with no damage, as long as no lateral bending moment was applied.

## 2.1 Disassembly of the LTAs

Disassembly was performed by placing the LTAs (hold-down plates with eight TPBARs and 16 thimble plugs) into a jig to support the LTA vertically. Clamps were then placed on the individual TPBARs to prevent them from dropping when the nuts holding the TPBARs to the hold-down plates were removed. A photo of LTA 8TR004 supported in the disassembly jig is shown in Figure 4. The nuts were easily removed and the TPBARs could be seen to drop easily away from the hold-down plate (about a

1-inch drop). This indicates minimal corrosion of the nuts and the area where the upper end plugs were inserted through the hold-down plates.

After the nuts for all eight TPBARs were removed, the hold-down plate with thimble plugs still attached was lifted away from the TPBARs. Fixtures were then attached to the upper end plugs of the TPBARs to facilitate handling and movement within the hot cell. Each TPBAR was then lifted out of the disassembly jig and placed into a storage container. A visual examination was performed at this time using binoculars through the hot cell window, which allowed the serial numbers of the individual TPBARs (on the upper end plug) to be read.

During this phase of the operations, the TPBARs appeared to hang straight with no visually apparent bow. There were no apparent significant defects or failures in the TPBARs. Noticeable features of the TPBARs included the following:

- Variations in the gray oxide layer on the exterior of the cladding.
- Axial scratches in the oxide from handling of the TPBARs at WBN and ANL-W.
- A circumferential region of differing appearance ~18 inches above the bottom of the TPBARs. This formation came to be called the "18-inch region" on the TPBARs. Figure 5 shows a photo of the 18-inch region, as observed during disassembly. This region appears to be a deposit that relates to changing flow conditions in the guide tube. (A coolant entrance hole and the top of the guide tube dashpot region are in this general location.) The extent and axial location of the 18-inch region varied from TPBAR to TPBAR. The later composite photography and detailed visual examination (see Section 2.2) better depicted this region.

A surface swipe of the deposits in the 18-inch region was taken on TPBAR T0166. Subsequent analysis for elemental and isotopic composition indicated that it was apparently reactor coolant system "crud." Further discussion of analyses of swipes taken during the NDE is presented in Section 3.7.2 of Lanning and Cunningham (2001).

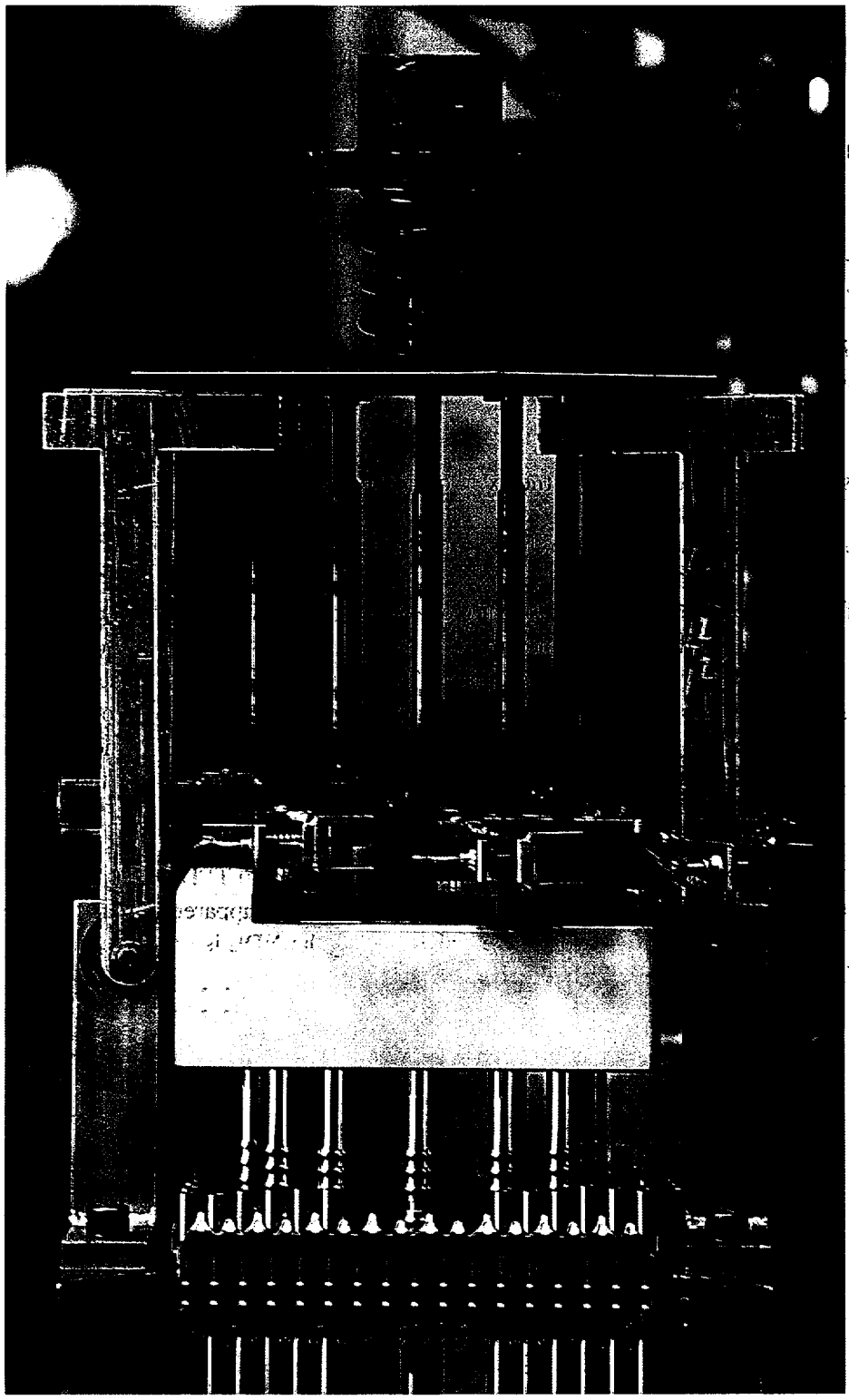

**Figure 4.** LTA 8TR004 in Disassembly Jig (Photo DD12224e)

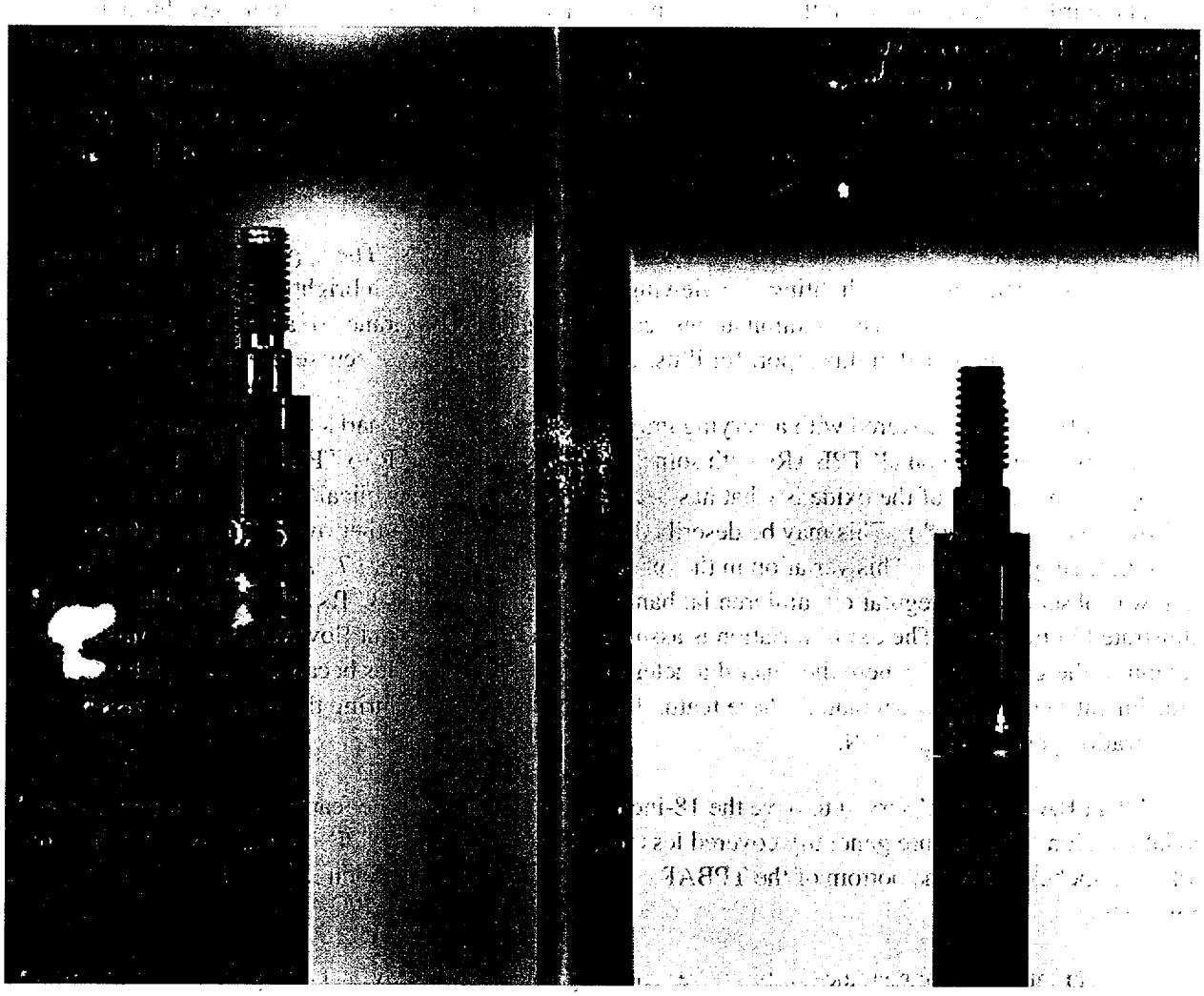

**Figure 5.** 18-Inch Region on TPBAR T0263 as Observed during LTA Disassembly (Photo T0263#1.8)

## 2.2 Visual Examination of the TPBARs

Visual examination of the TPBARs at ANL-W was performed in several phases. The first phase was during the disassembly of the LTAs, as described earlier. This examination was done through the hot cell windows using the naked eye and binoculars. Digital photography was used to document some aspects of the examination. All components were found to be covered with an adherent gray oxide. The identification numbers on the hold-down plates were clearly readable.

The second examination was composite photography. Each TPBAR was digitally photographed along its full length at 0°, 120°, and 240°. Prints were prepared at near 1:1 scaling, with each print covering ~11 inches of TPBAR length. Prints and compact disks of the digital files were provided to PNNL. The prints were also used by ANL-W staff to identify potential features for additional detailed visual examination and photography.

The third examination was at the visual examination station using digital photography through a periscope. This provided views up to a magnification of approximately 10X. The entire surface of each TPBAR was viewed (the TPBARs were lifted while being rotated), but photos were taken only of selected features. PNNL participated in the examination of the first TPBAR (T0256) to provide guidance to ANL-W for the balance of the examinations. Prints of selected features, plus compact disks with files of all photographs taken, were provided to PNNL.

A variety of features were observed during the visual examinations. The appearance of the features often varied depending on the lighting and viewing technique; a change in brightness or direction of the lighting (during any of the visual examinations) could change the appearance of a feature. Selected photos have been included in this report for illustration and example, as discussed below.

All TPBARs were covered with a varying gray oxide, and handling marks (scratches in the oxide) were easily observable on all TPBARs with some variation from TPBAR to TPBAR. See Figure 6 for an example. One feature of the oxide is what has been characterized as a cyclical/helical variation (also referred to as "chevrons"). This may be described as a brighter region either overlaying or underlying the more normal gray oxide. This variation in the oxide is illustrated in Figure 7. Another oxide variation that was observed was regular circumferential bands at the top of the TPBARs and the thimble plugs as illustrated in Figure 8. The oxide variation is assumed to be due to coolant flow variations in this region of the guide tubes where the inner diameter of the guide tube varies because of the mechanical attachment to the hold-down plate. These features were also observed during the underwater visual observation performed at WBN.

All TPBARs were observed to have the 18-inch-region feature, but the feature varied in intensity and axial location. The feature generally covered less than an axial inch of a TPBAR and was generally from 14 to 22 inches above the bottom of the TPBARs. Illustrations of the 18-inch region are provided in Figure 9.

An example of the appearance of the lower end plug and weld is provided in Figure 10. In this figure, the photo on the left was taken during composite photography. It shows that oxide had rubbed off the TPBARs in the lower end plug weld region and deposited on the tray used to support the TPBARs during this examination. This is an indication that the oxide, while highly adherent, can be removed through metal-to-metal contact. All lower end plugs looked satisfactory and no unusual features were observed. The view on the right in Figure 10 was taken during detailed visual examination.

A feature characterized as a "circular mark" was observed on some TPBARs. This mark was similar to the 18-inch region, but was more limited and appeared as a small circle. An example of this feature is shown in Figure 11. The feature usually occurred at about 22 inches and at 140-143 inches above the bottom of a TPBAR. These positions generally correspond with the axial position of the fuel assembly grid structures, so it is postulated that the markings are the result of guide tube internal features resulting from the fabrication of the fuel assembly structure (that is, they result from a change in flow characteristics within a guide tube and are probably crud deposits).

During attachment of the TPBARs to the hold-down plates at Westinghouse's Columbia facility, a circumferential scratch was observed on TPBAR T0256. This scratch was ~0.0018 inches deep by

0.125 inches long, and analysis concluded that it did not impact the structural integrity of the TPBAR. The scratch was ~37 inches above the bottom of the TPBAR. This scratch was examined during the visual examinations and photos are provided in Figure 13. The postirradiation appearance of this scratch was very similar to the pre-irradiation appearance; thus, the scratch was apparently not impacted by the irradiation.

Although a variety of features were noted on the surface of the TPBARs, there was no indication that these features had any impact on the TPBARs.

**Figure 6.** Example of Handling Scratches, TPBAR T0256 (Photo 2560#2)

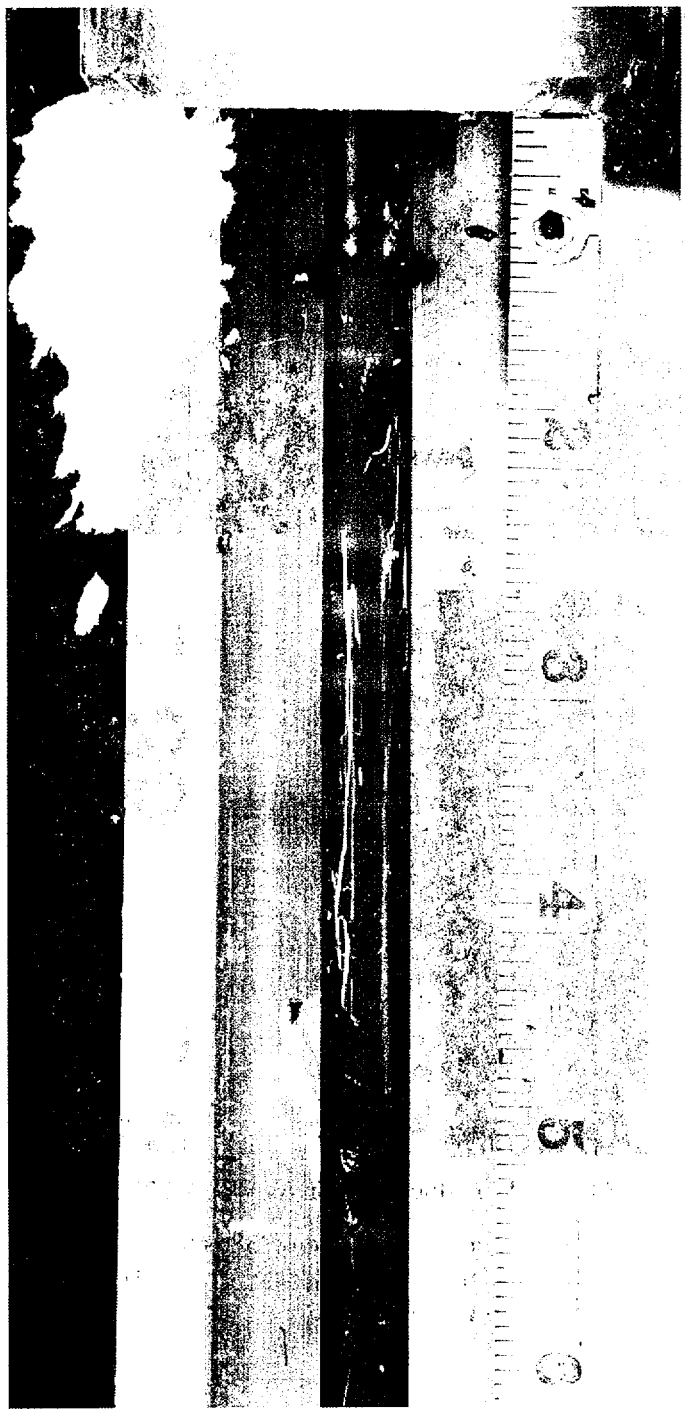

**Figure 8.** Example of Light Gray Oxide Bands at Top of TPBAR T0238 (Photo 2380#1)

**Figure 7.** Example of Cyclical/Helical Oxide Appearance, TPBAR T0256 (Photo 2560#8)

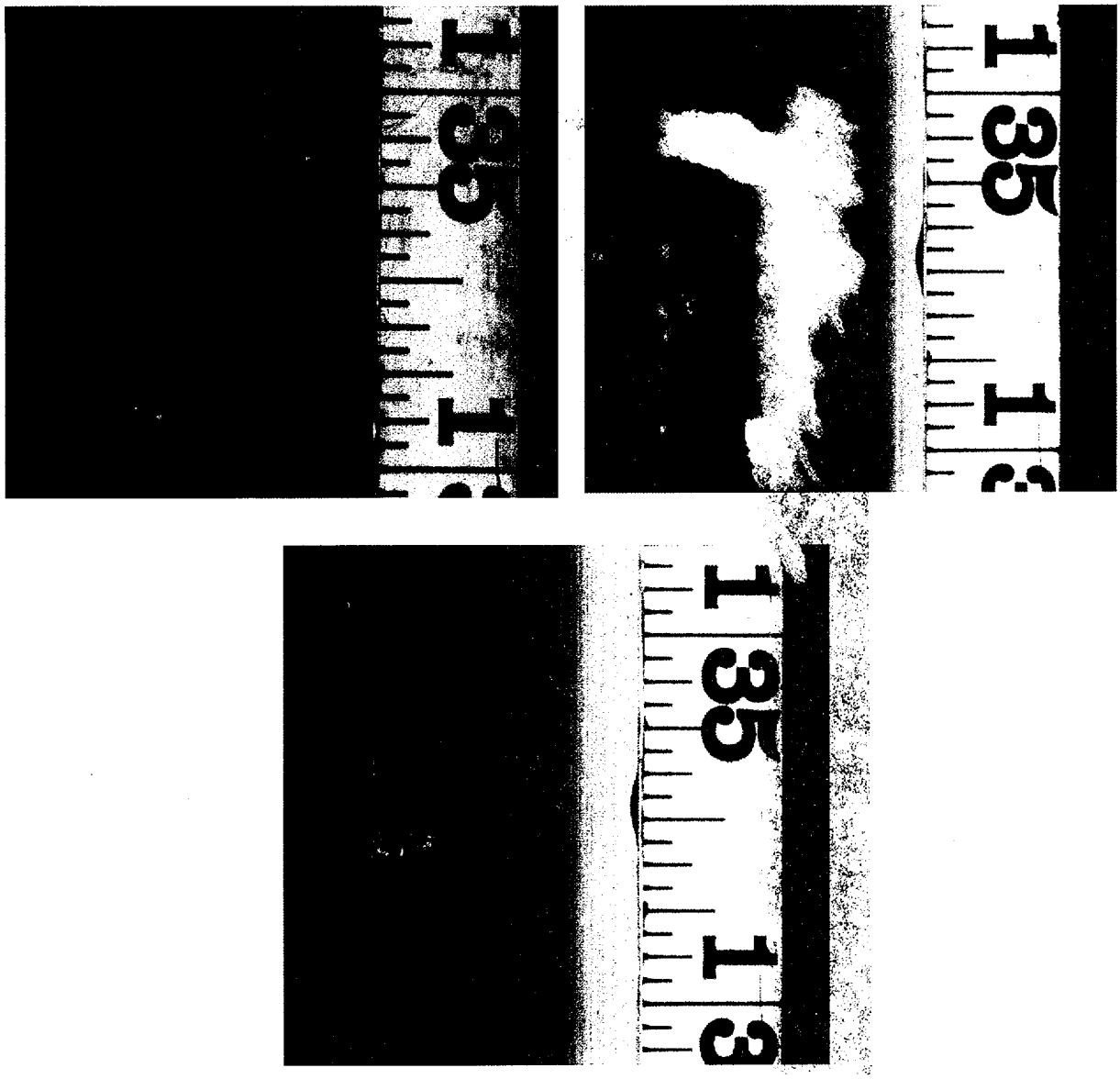

**Figure 9.** 18-Inch Region on TPBAR T0238

Upper Left: 0° (Photo 2380#14);
Upper Right: 120° (Photo 238120#14);
Lower: 240° (Photo 238240#14).

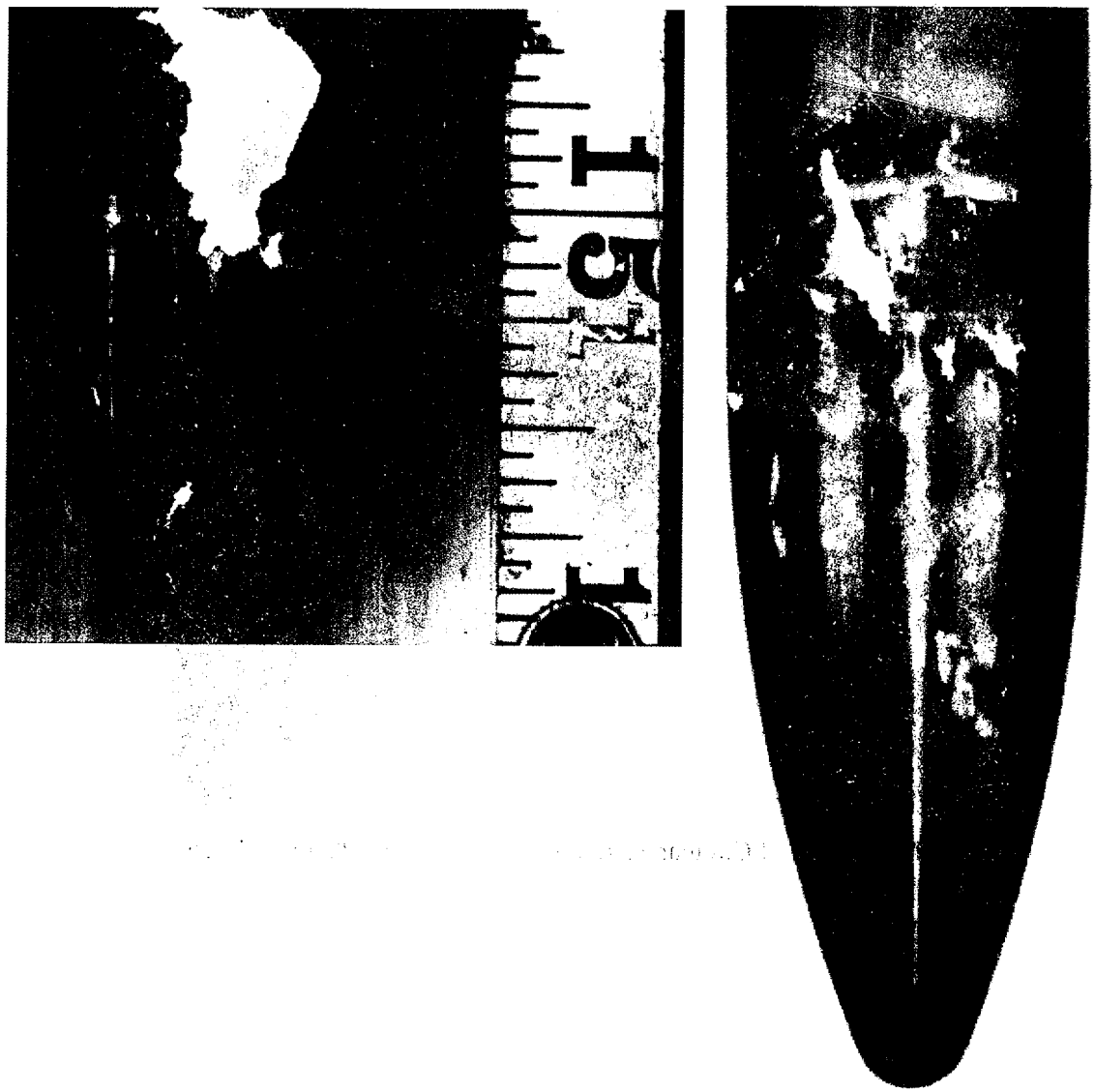

**Figure 10.** Examples of End Plug Weld Condition at End of Irradiation
(Left, Photo 2380#16; Right, Photo VEM 256#27)

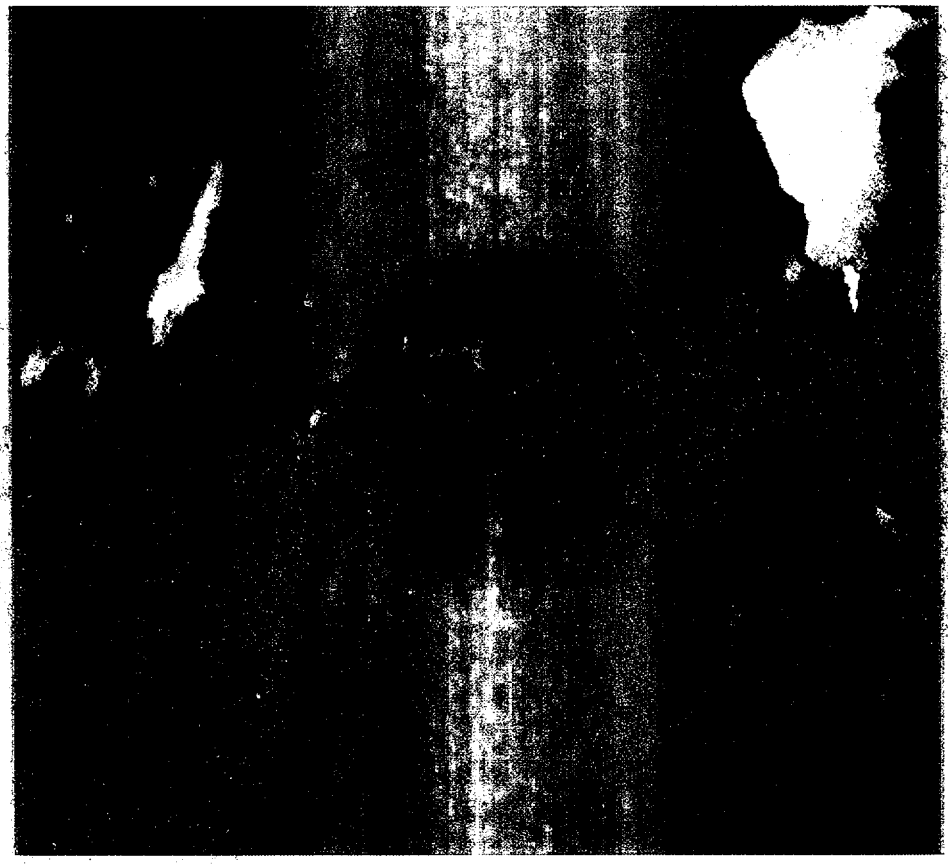

**Figure 11.** Example of Circular Mark on TPBAR T0256 (Photo VEM 256#24)

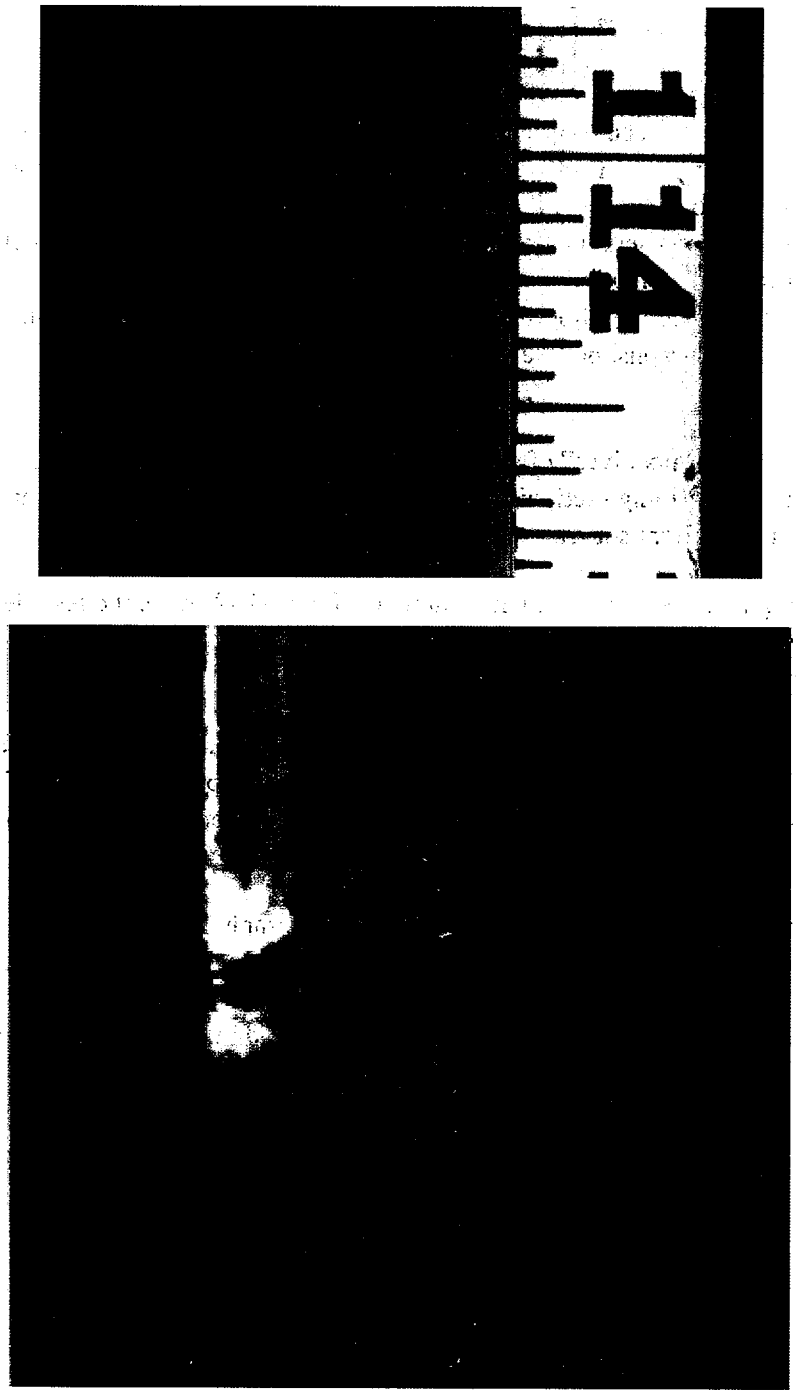


**Figure 12.** Photographs of Circumferential Scratch on TPBAR T0256 at 37 Inches

Top Photograph from Composite Photography (Photo 2560#12).
Bottom Photograph from Visual Examination (Photo VEM 256 #32).

## 2.3 Neutron Radiography

To conduct the neutron radiography, two TPBARs at a time were inserted into individual tubes and placed onto a carrier. After the neutron exposure, a foil pack was removed and the activated foils were placed in contact with unexposed camera film to expose the film. The exposed film was then developed to produce the neutron radiographs. Dysprosium-exposed films represent the thermal neutron radiographs and indium-exposed films represent the epithermal neutron radiographs. An axial scale can be seen on the dysprosium, thermal neutron radiographs, but not on the indium, epithermal neutron radiographs. The reason for the two neutron energy radiographs is that the pellets are more apparent in the epithermal than in the thermal neutron radiographs, but the scale and other TPBAR features are visible in the thermal neutron radiographs.

In addition to the films, "positives" of the films were made for TPBARs T0166, T0195, T0281, and T0291 for PNNL's use in defining sectioning positions for the DE. The positives were made by exposing the films to a high-intensity light source.

All neutron radiographs were labeled with a number (for ANL-W use), the test identification, the elevation of the radiograph, and the TPBAR identification. The first TPBAR number was for the bottom image and the second TPBAR number was for the top image.

As previously noted, to radiograph the entire length of the TPBARs, it was necessary to invert the TPBARs, and PNNL reviewed the neutron radiography for the first pair of TPBARs (T0207 and T0209) at ANL-W. Because there was no observable axial shifting of the pencil column from the inverting process, PNNL authorized the inverting process for all remaining TPBARs.

A number of features were evident from the neutron radiography that are relevant to the performance of the TPBARs. It was expected that the TPBAR cladding would not fail during the irradiation. The neutron radiography displayed no evidence of free moisture in any TPBAR, thus providing evidence that the TPBAR cladding had not failed. This conclusion that the cladding was intact for every TPBAR was confirmed by the rod puncture and gas analysis conducted later.

It was expected that the pellet material, which is a neutron absorber, would not relocate during the irradiation. Relocation of the absorber material could result in unacceptable local power peaking. Relocation could occur from either pencil movement that opened axial gaps between the pencils, or pellet cracking that could cause pellet pieces to fall out of the pencils.

No gaps between pencils were observed in the neutron radiography. Thus, there was no apparent axial movement of the pencils during the irradiation or subsequent handling and shipping. This observation also correlates with the observed difficulty of removing getters from cut sections during the DE of the target rods irradiated in the Advanced Test Reactor (ATR) (Lanning et al. 1999).

A substantial number of pellets were observed to be cracked, but the general structure of the pellets was maintained between the getter and liner, as expected. Many bottom pellets in a pencil were observed to be circumferentially cracked about 0.1 inch above the bottom of the pellet. This observation of cracking conforms with observations of pellet cracking that occurred during the getter coining operation

of pencil fabrication. Other cracks likely occurred during fabrication also because of high loads during pencil coining.

A few TPBARs (T0281, T0266, T0165, T0232, T0263, T0169, T0183, T0262) showed some evidence of a little pellet debris falling out of a pencil and moving to the bottom of the TPBAR. It was apparent that the debris came from the upper pellet in a pencil stack and from the upper edge of the pellet where the inner liner did not capture the pellet piece after it broke. It is not possible to determine if the pellet broke during fabrication or handling, but fabrication is suspected. The quantity of pellet material observed was small; the largest observed quantity was an approximately conical shaped pile with a base diameter equal to the inside diameter of the liner and a height of ~0.1 inch. This material was apparently free to move down the inside of the pencil column, because the broken pellet material in some of the TPBARs also was observed at the top of the pencil column in the inverted neutron radiography.

An unexpected observation on the mechanical integrity of the pencils was that the liner was commonly observed to extend from the top of a pencil into the bottom of the next higher pencil in the column. This occurrence was observed as a thin line in the pencil-pencil interface on the inside of the pellets. This was not an expected observation because the pencils were designed to accommodate liner growth, but apparently not the amount that was observed. Further discussion of pencil and liner length changes is provided in Section 2.8.2. Although this behavior was evaluated, it had no apparent impact on the in-reactor performance of the TPBARs.

The neutron radiographs also provided information on the tritium and hydrogen distribution within the TPBARs because, first, tritium decays in place to He-3, which is a very good neutron absorber; and, second, because hydrogen isotopes are good neutron scatterers. Tritium (He-3) absorption is apparent as bright spots, while neutron scatter is more apparent as a bright fogging.

## 2.4 Axial Gamma Scanning

Axial gamma scanning and spectral analyses were performed on all 32 TPBARs. Two of the TPBARs designated for DE, T0291 and T0195, were scanned in 0.1-inch steps along the full length, from ~12 inches below the shoulder on the upper end plug to the bottom end plug. The other 30 TPBARs were scanned in 0.1-inch steps across a 12-inch span in the midplane (70 to 82 inches from the shoulder), which did include the pencil-6-to-pencil-7 interface. All scanning was done with equal slit width (0.1 inch), counting time (300 seconds), and distance from aperture to TPBAR, to provide same-basis qualitative comparisons between the TPBARs and axial positions.

Pencil-pencil interface locations were clearly discernible by peaks in the Co-60 activity levels. In addition, the lower end plug location was clearly discernible as a large Co-60 peak. These same scans have a large peak in the Nb-95/Zr-95 activity adjacent to and just above the Co-60 end plug peak, corresponding to the solid Zircaloy disk at that location. Except for these peaks, the activity was quite uniform (as predicted) along the majority of the TPBAR lengths. The activity of specific isotopes was also quite uniform among TPBARs, which is consistent with Westinghouse predictions of uniform tritium production (within 5% relative) among the TPBARs.

Finally, close inspection of the full-length Zr-95 and Nb-95 scans revealed that very little (<0.1 inch) separation of pencils occurred, even though the TPBARs had been inverted for neutron radiography and profilometry prior to gamma scanning. This is consistent with the observation of minimal pencil-pencil separation in the neutron radiographs.

## 2.5 Metrology

All TPBARs were measured for diameter (at five angles), for total length, and for bow. These measurements and results are discussed in the following sections.

### 2.5.1 TPBAR Diameter

TPBAR diameter measurements were taken with the TPBARs hanging freely from their end fittings, and all measurements are indexed from the shoulder of the upper end plug. The diameter scans began from ~12 inches below the upper end plug shoulder; the top 12 inches could not be measured because of physical limitations in the hot cell. The diameter measurements were recorded at 0°, 45°, 90°, 135°, and 180°, relative to the index pin of the TPBAR end fitting; this orientation is arbitrary for any specific TPBAR.

An example diameter plot for TPBAR T0291 is provided in Figure 13. The average diameter for all TPBARs is provided in Table 4. Except for a few cases, these values are within the as-fabricated specification of 0.3810 inch ±0.005 inch.

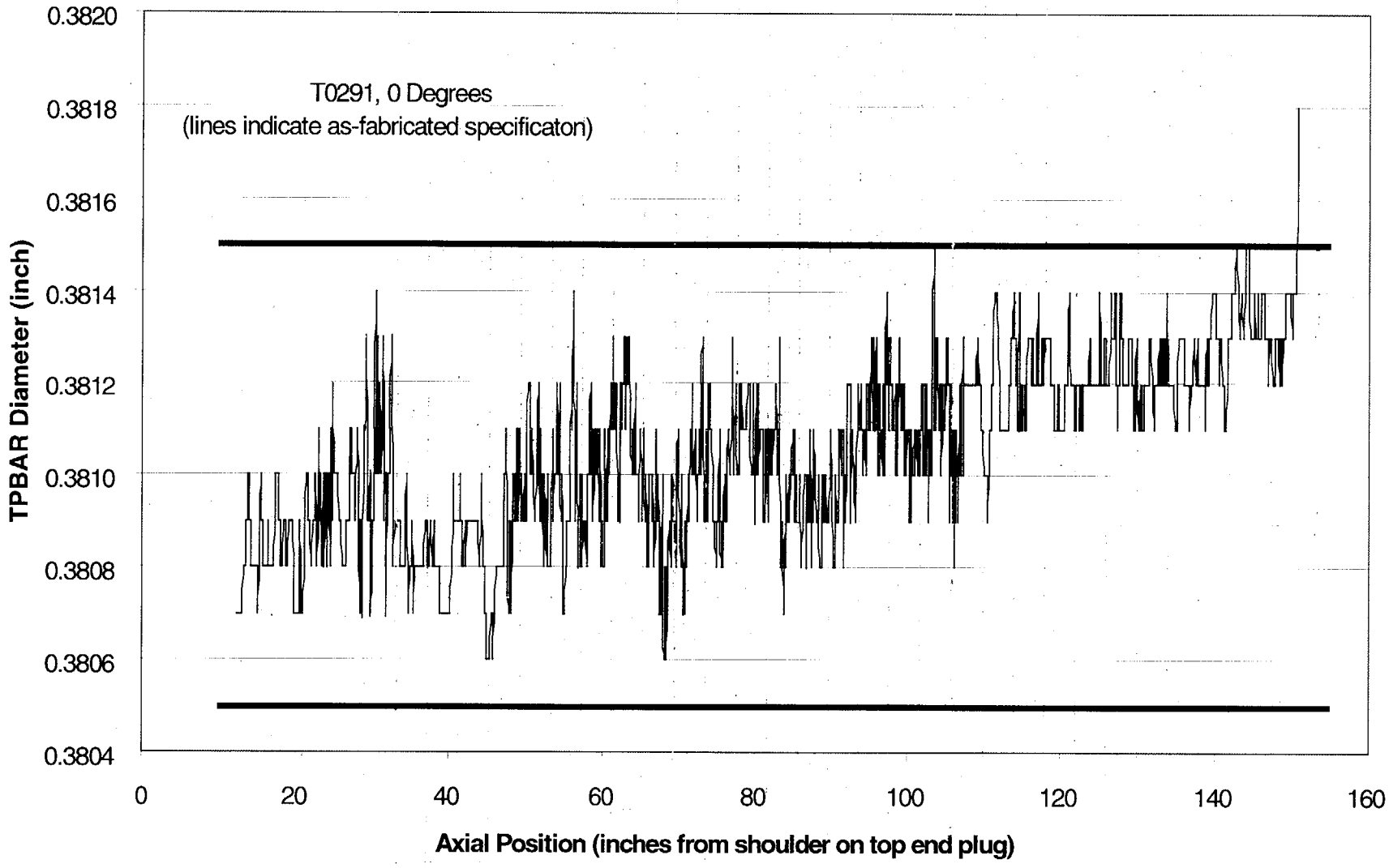


**Figure 13.** Diameter Plot for TPBAR T0291, 0°

**Table 4.** Summary of Average Postirradiation Diameter for the TPBARs

| TPBAR | Average Diameter at 0° (inch) | Average Diameter at 45° (inch) | Average Diameter at 90° (inch) | Average Diameter at 135° (inch) | Average Diameter at 180° (inch) |
|---|---|---|---|---|---|
| *LTA 8TR001* | | | | | |
| T0168 | 0.3812 | 0.3810 | 0.3811 | 0.3810 | 0.3809 |
| T0169 | 0.3810 | 0.3811 | 0.3813 | 0.3813 | 0.3810 |
| T0171 | 0.3810 | 0.3811 | 0.3809 | 0.3811 | 0.3811 |
| T0237 | 0.3810 | 0.3812 | 0.3813 | 0.3810 | 0.3811 |
| T0238 | 0.3811 | 0.3812 | 0.3812 | 0.3812 | 0.3812 |
| T0256 | 0.3813 | 0.3816 | 0.3816 | 0.3816 | 0.3814 |
| T0281 | 0.3807 | 0.3808 | 0.3811 | 0.3811 | 0.3812 |
| T0291 | 0.3811 | 0.3810 | 0.3811 | 0.3811 | 0.3812 |
| *LTA 8TR002* | | | | | |
| T0165 | 0.3813 | 0.3812 | 0.3810 | 0.3811 | 0.3811 |
| T0176 | 0.3809 | 0.3811 | 0.3812 | 0.3810 | 0.3809 |
| T0202 | 0.3812 | 0.3813 | 0.3814 | 0.3815 | 0.3815 |
| T0215 | 0.3809 | 0.3811 | 0.812 | 0.3812 | 0.3811 |
| T0232 | 0.3811 | 0.3811 | 0.3816 | 0.3813 | 0.3813 |
| T0241 | 0.3810 | 0.3812 | 0.3812 | 0.3812 | 0.3812 |
| T0266 | 0.3811 | 0.3812 | 0.3813 | 0.3813 | 0.3813 |
| T0287 | 0.3810 | 0.3810 | 0.3811 | 0.3815 | 0.3815 |
| *LTA 8TR003* | | | | | |
| T0183 | 0.3810 | 0.3813 | 0.3811 | 0.3809 | 0.3811 |
| T0210 | 0.3810 | 0.3810 | 0.3810 | 0.3809 | 0.3809 |
| T0217 | 0.3812 | 0.3812 | 0.3811 | 0.3813 | 0.3811 |
| T0225 | 0.3810 | 0.3811 | 0.3812 | 0.3810 | 0.3812 |
| T0260 | 0.3809 | 0.3812 | 0.3811 | 0.3809 | 0.3811 |
| T0262 | 0.3812 | 0.3811 | 0.3809 | 0.3811 | 0.3811 |
| T0277 | 0.3813 | 0.3815 | 0.3816 | 0.3815 | 0.3814 |
| T0290 | 0.3810 | 0.3808 | 0.3808 | 0.3810 | 0.3809 |
| *LTA 8TR004* | | | | | |
| T0166 | 0.3811 | 0.3812 | 0.3812 | 0.3813 | 0.3813 |
| T0195 | 0.3808 | 0.3809 | 0.3809 | 0.3810 | 0.3810 |
| T0205 | 0.3810 | 0.3809 | 0.3810 | 0.3809 | 0.3811 |
| T0206 | 0.3814 | 0.3815 | 0.3815 | 0.3815 | 0.3815 |
| T0207 | 0.3810 | 0.3811 | 0.3812 | 0.3811 | 0.3812 |
| T0209 | 0.3811 | 0.3811 | 0.3811 | 0.3811 | 0.3810 |
| T0261 | 0.3811 | 0.3811 | 0.3812 | 0.3812 | 0.3813 |
| T0263 | 0.3811 | 0.3811 | 0.3811 | 0.3812 | 0.3812 |

### 2.5.2 TPBAR Length and Bow

TPBAR length and bow measurements were taken with the TPBARs hanging freely from their end fittings. All measurements were indexed from the shoulder of the upper end plug, so the total length of the TPBARs is the recorded length plus 0.670 inch for the threaded portion of the upper end plug. The TPBAR bow scans begin from ~12 inches below the upper end plug shoulder; the top 12 inches could not be measured because of physical limitations in the hot cell. The position of the TPBAR was measured in three-dimensional space at a number of axial locations, typically at 10-inch increments along the length.

Rod bow is defined as the distance from the theoretical rod tip-to-tip centerline to the rod's centerline at any axial position along the TPBAR, where the tip-to-tip centerline was inferred from the bow and length data.

The vertical length was determined by touching the bottom tip of the TPBAR to a conductive plate and then comparing that Z-position to the Z-position of a similarly positioned length standard. The bowed length was calculated by summing segment lengths (from measurement to measurement) between the three-dimensional positions of the TPBAR centerline.

TPBAR length and bow measurements are summarized in Table 5. The length measurements are graphically shown in Figure 14, and the bow measurements are graphically shown in Figure 15. In addition, bow as a function of TPBAR axial position is presented in Figure 16 for TPBARs T0166, T0195, T0281, and T0291.

No direct pre-irradiation measurements of TPBAR length were made; the TPBARs were checked only to see that they met the specification. In Figure 14, measured postirradiation TPBAR length is compared to the fabrication specification (151.70 inches equals the total length of 152.37 inches minus the shank length of 0.670 inches) and the calculated design bound of postirradiation length. The measured postirradiation length for the TPBARs is greater (by up to 0.08 inch) than the upper tolerance of fabrication and less than the postirradiation length that was acceptable for the design.

From Table 5 and Figure 15, it can be seen that the TPBAR bow ranged from ~0.1 to 0.4 inch. This agrees well with the qualitative observations of minimal bow from the visual examinations and the neutron radiography.

Figure 16 shows that maximum bow usually occurred from about 60 to 80 inches below the top of the TPBARs.

**Table 5.** Summary of TPBAR Length and Bow Measurements

| TPBAR | Vertical Length (inch) | Bowed Length (inch) | Maximum Bow and Axial Distance from TPBAR Top (inch) |
|---|---|---|---|
| *LTA 8TR001* | | | |
| T0168 | 151.761 | 151.771 | 0.267 at 62.21 |
| T0169 | 151.790 | 151.795 | 0.262 at 62.19 |
| T0237 | 151.793 | 151.795 | 0.101 at 108.90 |
| T0238 | 151.826 | 151.828 | 0.291 at 68.89 |
| T0256 | 151.804 | 151.806 | 0.205 at 62.19 |
| T0171 | 151.777 | 151.780 | 0.268 at 62.20 |
| T0281 | 151.784 | 151.796 | 0.235 at 78.89 |
| T0291 | 151.781 | 151.797 | 0.146 at 88.89 |
| *LTA 8TR002* | | | |
| T0165 | 151.780 | 151.785 | 0.179 at 98.90 |
| T0176 | 151.761 | 151.763 | 0.370 at 78.92 to 88.91 |
| T0202 | 151.776 | 151.780 | 0.348 at 78.90 |
| T0215 | 151.761 | 151.769 | 0.438 at 88.90 |
| T0232 | 151.763 | 151.772 | 0.270 at 98.89 |
| T0241 | 151.771 | 151.779 | 0.122 at 78.89 to 88.90 |
| T0266 | 151.777 | 151.786 | 0.165 at 88.89 |
| T0287 | 151.761 | 151.765 | 0.235 at 88.89 |
| *LTA 8TR003* | | | |
| T0183 | 151.760 | 151.766 | 0.133 at 62.20 |
| T0210 | 151.754 | 151.766 | 0.191 at 138.89 |
| T0217 | 151.758 | 151.761 | 0.380 at 68.89 |
| T0225 | 151.764 | 151.773 | 0.344 at 78.89 |
| T0260 | 151.774 | 151.781 | 0.180 at 78.89 |
| T0262 | 151.776 | 151.786 | 0.359 at 78.90 |
| T0277 | 151.780 | 151.786 | 0.238 at 68.89 |
| T0290 | 151.764 | 151.768 | 0.372 at 78.89 |
| *LTA 8TR004* | | | |
| T0166 | 151.780 | 151.788 | 0.360 at 68.79 |
| T0195 | 151.753 | 151.768 | 0.192 at 52.22 to 62.21 |
| T0205 | 151.781 | 151.791 | 0.295 at 58.89 to 62.21 |
| T0206 | 151.798 | 151.802 | 0.383 at 69.90 |
| T0207 | 151.739 | 151.759 | 0.286 at 62.18 |
| T0209 | 151.770 | 151.783 | 0.139 at 52.20 |
| T0261 | 151.781 | 151.804 | 0.301 at 62.21 |
| T0263 | 151.759 | 151.771 | 0.355 at 62.19 |

NOTE: Lengths are from upper end plug shoulder to tip of lower end plug and do not include threaded portion of the upper end plug.
Axial position of maximum bow is relative to upper end plug shoulder.
Angles for bow measurements are provided in the data transmittals from ANL-W. However, they are not reported here because the angles relate to arbitrary installation positions in the handling fixtures and are not related to in-reactor orientations.

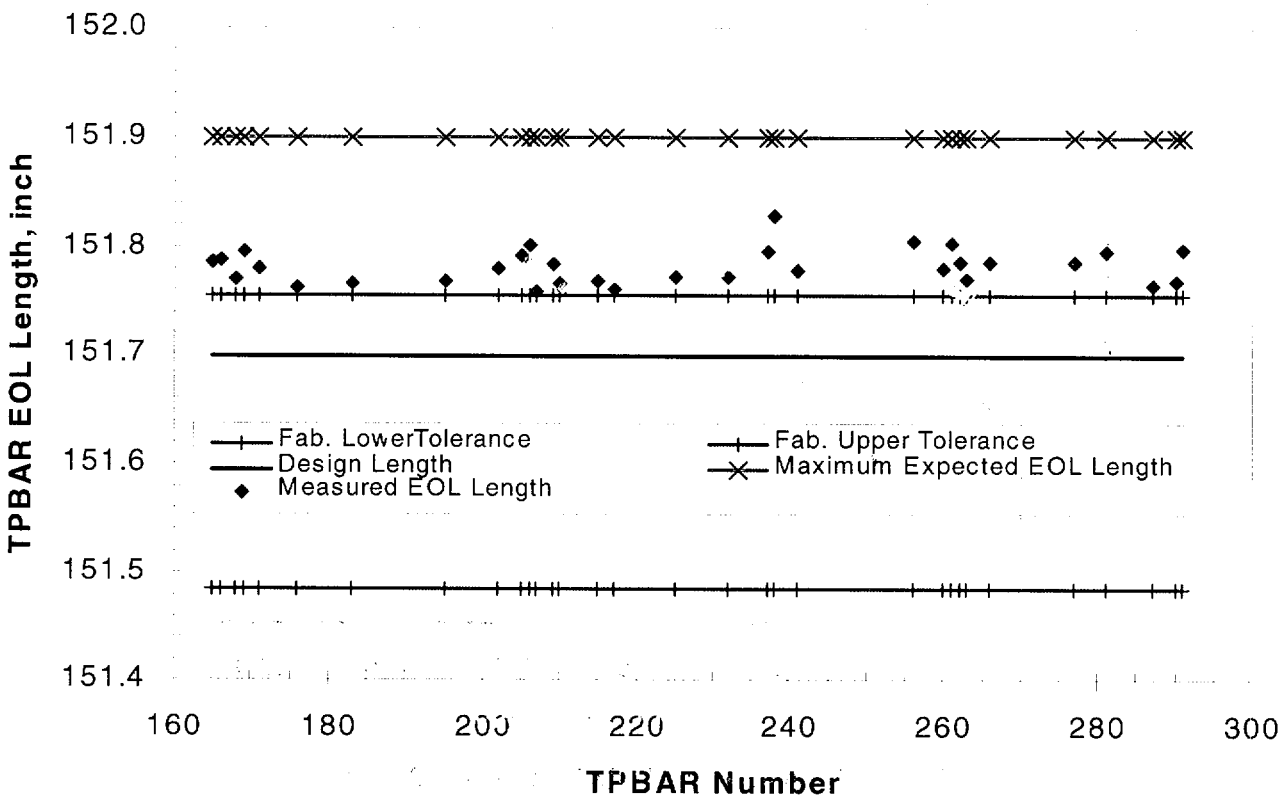


**Figure 14.** Summary of TPBAR Length Measurements with Comparison to Pre-Irradiation Specification

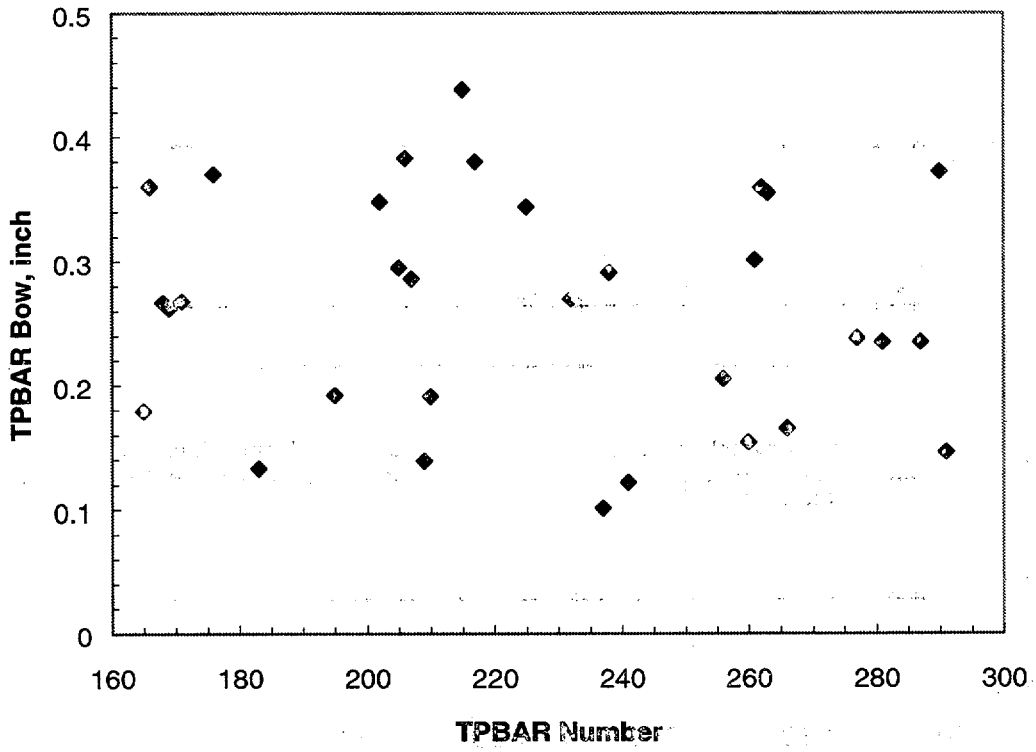


**Figure 15.** Summary of TPBAR Maximum Bow Values

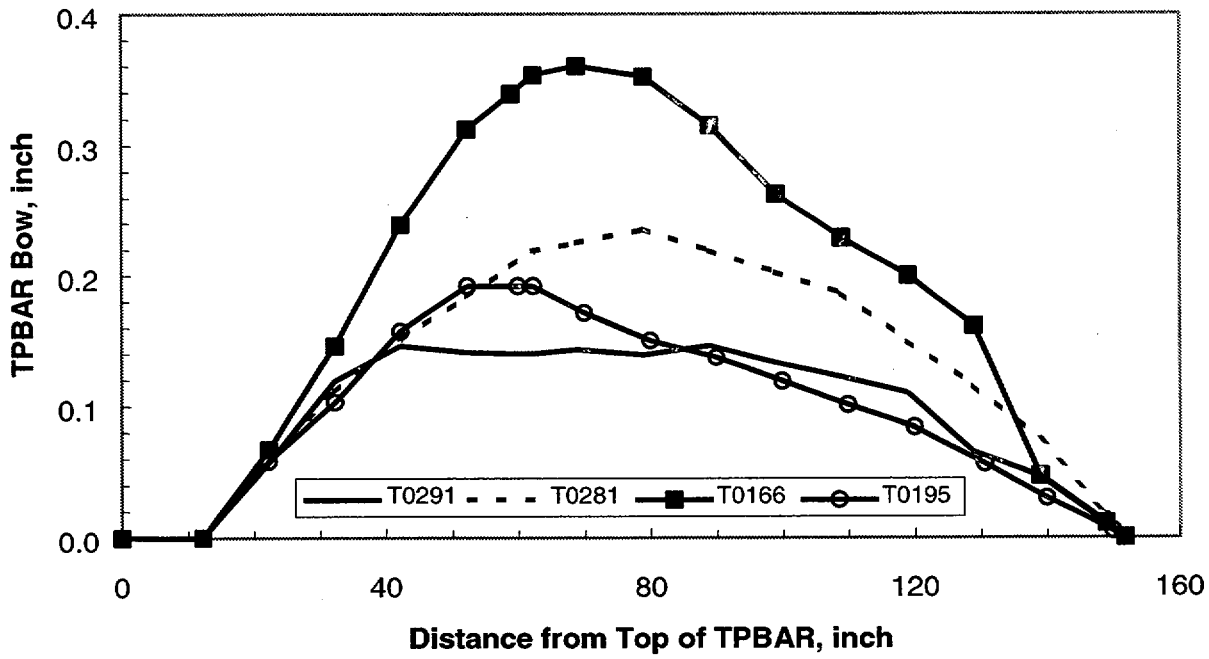


**Figure 16.** Example of TPBAR Bow

## 2.6 Rod Puncture and Gas Analysis

ANL-W's Gas Analysis, Sample, and Recharge (GASR) system was used to puncture the TPBARs, collect gas for composition analysis, and measure both TPBAR internal gas pressure at the time of puncture and TPBAR internal void volume. PNNL provided to ANL-W four test articles of prototypic pressure and gas volume for qualification of the GASR system. These test articles allowed ANL-W to demonstrate that adequate adjustments had been made to the GASR system, since the TPBARs would hold a greater quantity of gas than rods normally handled by the system. Satisfactory comparisons of as-built conditions and as-measured puncture results were also obtained on the test articles prior to puncturing the first TPBAR.

The TPBAR puncturing and gas analysis provided the definitive evaluation of whether the TPBARs were intact after irradiation and shipping. All TPBARs had the expected irradiation-induced pressurization levels, and the gas compositions indicated no failure of the TPBARs. Oxygen concentrations, when significant, occurred in conjunction with nitrogen concentrations that indicated air inleakage into the gas samples, not air or water inleakage to the TPBARs. Therefore, it may be concluded that all 32 TPBARs successfully survived the irradiation and subsequent shipping with no cladding failures.

### 2.6.1 Rod Puncture, Void Volume, Gas Pressure

The TPBARs were punctured in the upper plenum region above the upper getter disk using a laser. The laser punched a small hole ~0.005-0.010 inch in diameter through the cladding. A sample line from the GASR system allowed a quantity of gas to be collected (outside the hot cell) in sample bottles for subsequent gas composition analysis. A series of backfills and expansions using helium were performed to determine the TPBAR void volume. After this work was done, no attempt was made to backfill the TPBARs or to reweld the puncture hole; thus, the internal atmosphere became a mixture of helium from the irradiation and backfills, and of argon from the hot cell atmosphere.

The measured gas pressures and void volumes were quite uniform across all 32 TPBARs. This supports the predicted uniformity in the TPBAR design and fabrication, in the irradiation conditions, and in tritium production.

The GASR gas lines were cleaned between punctures using a PNNL-recommended gas mixture of hydrogen-doped argon (Ar-0.01%H2) to remove residual tritium that might impact subsequent gas collection and analysis.

### 2.6.2 Gas Composition Analysis

Gas composition and isotopic helium analyses were performed using a VARIAN-MAT model CH7 magnetic sector mass spectrometer. The evacuated cylinders were filled with plenum gas sampled by attaching them to an out-of-cell gas sampling port connected to the in-cell GASR system. Ambient (out-of-cell) temperature was monitored during the collection process, and the out-of-cell portion of the

system was maintained by controlled gas expansion to be significantly sub-atmospheric pressure (~5 psia) during the sample collection process. This mitigated the potential for out-of-cell spread of tritium-contaminated gas, but introduced the potential for air inleakage into the sample.

The cylinders containing the gas samples were then transported to the analysis laboratory and attached to a part of the mass spectrometer inlet system attached to an MKS Baratron capacitance manometer (certified by the National Institute of Standards and Technology [NIST]). The sample gas was then expanded in a series of steps prior to the analysis. Data was collected and reduced and the system was controlled by a personal-computer-based data acquisition system. Calibration of the system-control software was done with pure NIST-traceable gases.

Isotopic scans were performed directly by the data acquisition system software. The isotopic scan routine of the data acquisition software assumed no bias effects exist for isotopes of the same element. However, results of calibration work determined that a significant bias existed (about 10% to 15%) in the helium mass range (He-3 relative to He-4), and this was attributed to the electron multiplier bias. Therefore, reported isotopic helium atom percents and ratios were derived from summing and renormalizing the helium gas composition results. Instrument composition calibration used pure He-3 and pure He-4 gases, and treated those isotopes as independent gas types. This corrected for the observed bias because instrument calibration for gas composition does incorporate ionization efficiency and multiplier bias for each pure gas calibrated.

All TPBARs had the expected predominantly helium atmosphere. Samples from four TPBARs (T0207, T0215, T0241, and T0168) had small concentrations of nitrogen and oxygen. The ratio of oxygen to nitrogen was typical for air, which indicates slight inleakage of air during the collection or handling of these gas samples.

Tritium activity was measured in the gas collected immediately after puncture. Tritium activity also was measured in samples taken after helium backfill gas sat in the last-punctured TPBAR (T0266) for 1, 2, 3, and 4 weeks.

Evaluation of the gas pressure and gas composition data is provided in Section 2.8.1.

## 2.7 Other Examinations Performed by ANL-W

In addition to the examinations discussed previously, ANL-W also performed other examinations to support the PIE and to provide data to support operations at the production reactor and at the Tritium Extraction Facility being built at the Department of Energy Savannah River Site. This additional work consisted of segmenting the four TPBARs that were sent to PNNL; taking swipes of TPBAR surfaces to provide data on possible crud composition; performing gamma dose rate measurements on a TPBAR and hold-down hardware; and collecting a large volume of gas so that Savannah River staff could analyze it for the trace isotope Ar-39. The results of these examinations are provided in Lanning and Cunningham (2001).

## 2.8 Evaluations of the Nondestructive Data

The TPBAR gas puncture data permitted a calculation of the quantity of He-4 produced for each TPBAR and, therefore, the quantity of tritium produced in a TPBAR. The full-length axial gamma scans for relative Co-60 activity were used to estimate the axial distribution of the tritium production. These data-based tritium estimates are presented here, compared to the predicted tritium production, and later will be compared to the destructive assay data. Both the production of tritium and its distribution within the TPBARs appear to be consistent with their specified and expected performance, as discussed below.

### 2.8.1 Predicted Versus Measured Tritium/Helium Production

The 32 TPBARs were type-designated by their distance relative to the core center, with eight different designations (A through H) within the four symmetrically placed assemblies, as shown in Figure 3. Westinghouse provided end-of-cycle estimates for the total tritium production and axial distribution for each TPBAR designation.[2] The predicted total tritium production per TPBAR ranged from 0.88 g to 0.92 g tritium, which is a very narrow range.

The He-4 production (in moles per TPBAR) is equivalent numerically to the tritium production, because one atom of He-4 is produced along with each atom of tritium. The derived tritium production (converted to grams per TPBAR) is compared to the predicted tritium production for each TPBAR (provided by Westinghouse) in Table 6 and Figure 17. The agreement is very close, and appears to follow the position-dependent pattern predicted by Westinghouse (indicated by a least-squares-fit line through the data in Figure 17 having a slope of ~1.0). On average, the derived tritium production is about 2% greater than the predicted production. On a TPBAR-average basis, this derived tritium production corresponds to a lithium burnup of ~11%, a Li-6 burnup of ~50%, and a gas-volume ratio of ~145. This is the standard-temperature-and-pressure (STP) volume of gas produced per unit volume of pellet. These estimates were further confirmed for TPBAR T0291 by measurement and integration of the Li-6 burnup along the length of the TPBAR (see Section 3.5).

Measured He-3/He-4 ratios show a slight negative correlation with tritium production, as illustrated in Figure 18. This negative relationship is consistent with higher neutron flux resulting in both higher He-3 burnup and higher tritium production. It also is further indication that the measured He-3 is predominantly from He-3 produced and released during in-reactor operation, not during post-shutdown decay of tritium.

The tritium concentration in the collected gas was found to be consistent with design expectations.

[2] Letter from ML Travis, WesDyne Nuclear Development Program, to CK Thornhill, PNNL, "Tritium Production in the TBPAR LTAs," February 15, 2002, PD-02-0373.

**Table 6.** Derived and Predicted Tritium Production in LTA TPBARs

| TPBAR Number | Puncture-Derived Tritium Produced (g T) | Predicted Tritium Production* (g T) |
|---|---|---|
| T0165 | 0.905 | 0.893 |
| T0166 | 0.915 | 0.919 |
| T0168 | 0.911 | 0.904 |
| T0169 | 0.915 | 0.919 |
| T0171 | 0.922 | 0.880 |
| T0176 | 0.915 | 0.904 |
| T0183 | 0.912 | 0.904 |
| T0195 | 0.904 | 0.880 |
| T0202 | 0.906 | 0.893 |
| T0205 | 0.884 | 0.893 |
| T0206 | 0.921 | 0.919 |
| T0207 | 0.889 | 0.893 |
| T0209 | 0.906 | 0.920 |
| T0210 | 0.907 | 0.904 |
| T0215 | 0.937 | 0.919 |
| T0217 | 0.887 | 0.880 |
| T0225 | 0.931 | 0.920 |
| T0232 | 0.940 | 0.920 |
| T0237 | 0.899 | 0.904 |
| T0238 | 0.903 | 0.893 |
| T0241 | 0.913 | 0.880 |
| T0256 | 0.965 | 0.919 |
| T0260 | 0.893 | 0.893 |
| T0261 | 0.890 | 0.904 |
| T0262 | 0.902 | 0.893 |
| T0263 | 0.903 | 0.904 |
| T0266 | 0.919 | 0.904 |
| T0277 | 0.939 | 0.919 |
| T0281 | 0.904 | 0.893 |
| T0287 | 0.936 | 0.919 |
| T0290 | 0.937 | 0.919 |
| T0291 | 0.954 | 0.920 |

* Letter from ML Travis, WesDyne Nuclear Development Program, to CK Thornhill, PNNL, "Tritium Production in the TPBAR LTAs," February 15, 2002, PD-02-0373.

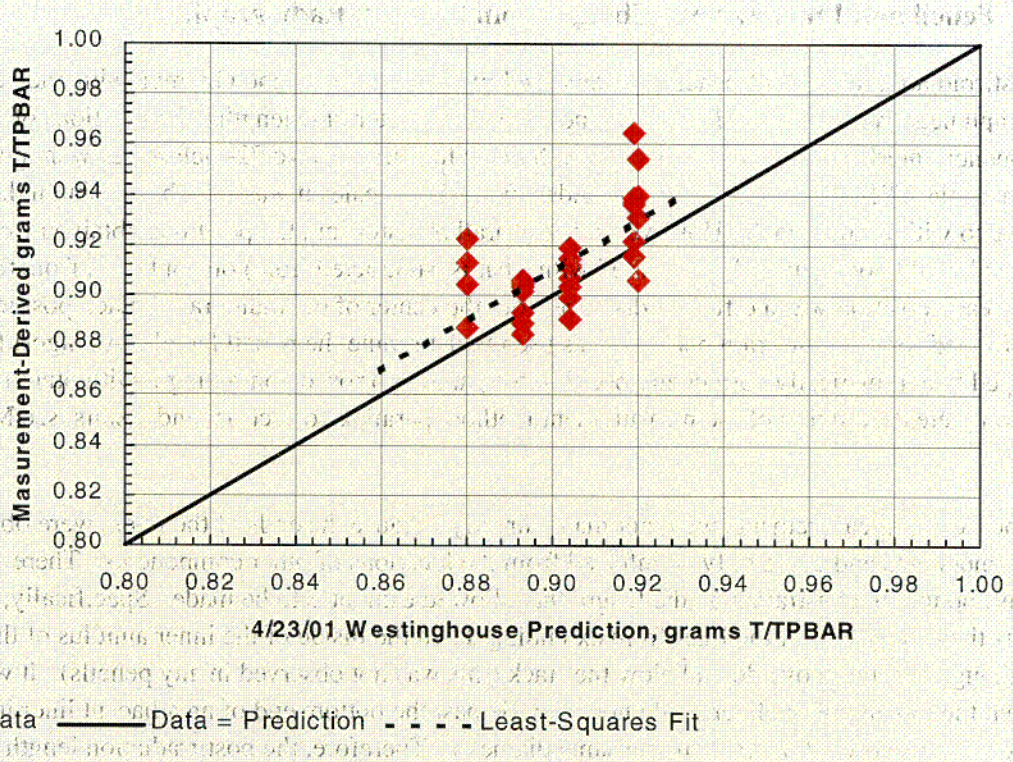


**Figure 17.** Derived Tritium Production (from TPBAR Puncture Measurements) Compared to Predicted Production

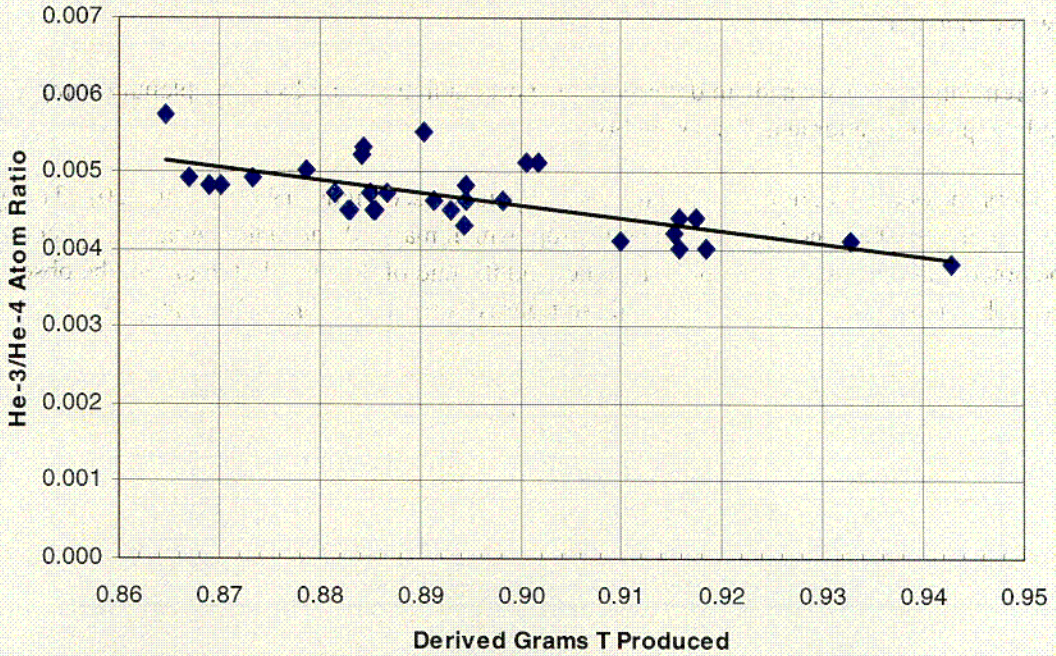


**Figure 18.** Comparison of He-3/He-4 Ratios to Estimated Tritium Production



L02

### 2.8.2 Pencil and Liner Length Change from Neutron Radiography

Postirradiation lengths of pencils (getters) and liners were determined by reviewing the neutron radiograph negatives for TPBARs T0166 and T0195. To determine lengths, the positions of the pencil-pencil interfaces were determined by reference to a scale. Two 72-inch scales were placed on-end adjacent to the TPBARs in the specimen holder; from these scales it was possible to obtain the position of a feature to within ±0.01 inch. However, due to parallax distortion, the positions obtained from one end of a pencil could not be directly combined with (that is, subtracted from) one obtained from the other end, because each position was a different distance from the center of the radiograph. Each position reading was corrected for this distortion before it was used to determine the pencil length. An algorithm was developed to automatically correct any position for parallax prior to combining it with other positions. For a complete description of the measurement method, parallax correction, and results, see McKee (2000).

Liner length measurements were not made directly because the ends of the liners were obscured by other components and could only be inferred from the locations of other components. There were, however, bounding constraints on the length that allowed estimates to be made. Specifically, the flange prevents the bottom end of the liner from extending down the inside of the inner annulus of the pellet stack, though it could move down below the stack (this was not observed in any pencils). It was also clear that the top end of the liner could not protrude past the bottom end of an adjacent liner in the next pencil down, because all liners were the same diameter. Therefore, the postirradiation length was determined for those liners in which the top end protruded past the top of the pellet stack. No uncertainty was calculated for these measurements because they were only estimates. The top of the liner was taken to be equal to the indication for the bottom of the pellet stack in the next pencil up, whereas the liner bottom was taken as the indication for the bottom of the pellet stack for the pencil in which the liner of interest was contained.

Measurements were also made to determine the postirradiation lengths of the plenum compression spring and the plenum getter and disk assembly.

The liners showed indications of growth in some pencils (see Figure 19 and Figure 20). This growth was observed only in the pencils located near the top, which may indicate a temperature dependency. It should be noted that, unless the liner protruded beyond the end of the pencil, it could not be observed in the radiographs. No error bars are shown in these figures as these data are only estimated.

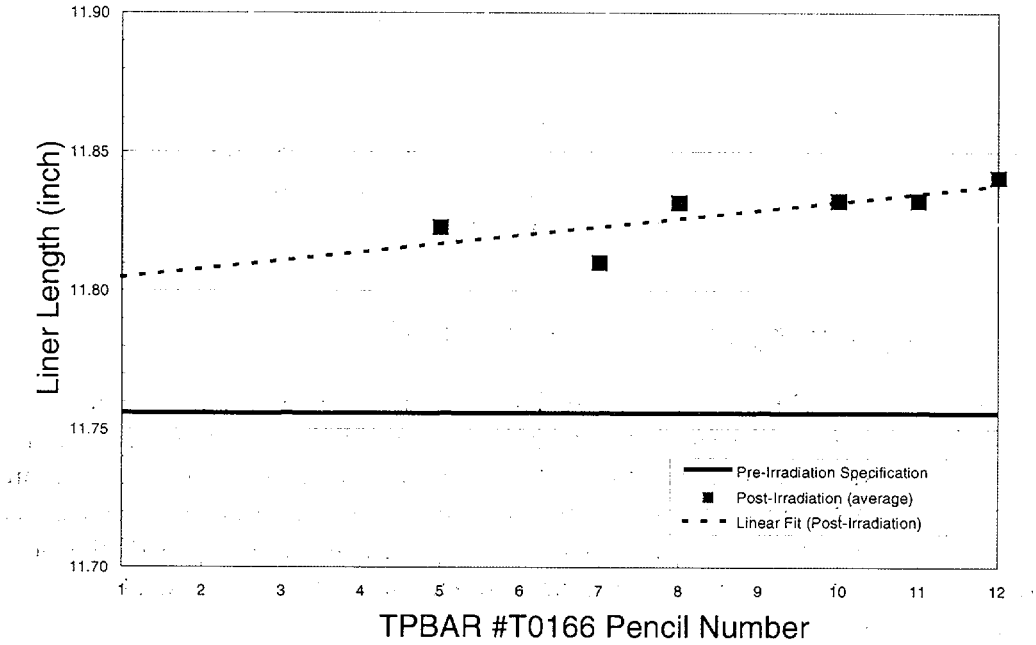


**Figure 19.** Comparison of Specified Pre-Irradiation Liner Length to Postirradiation Length Estimates for TPBAR T0166

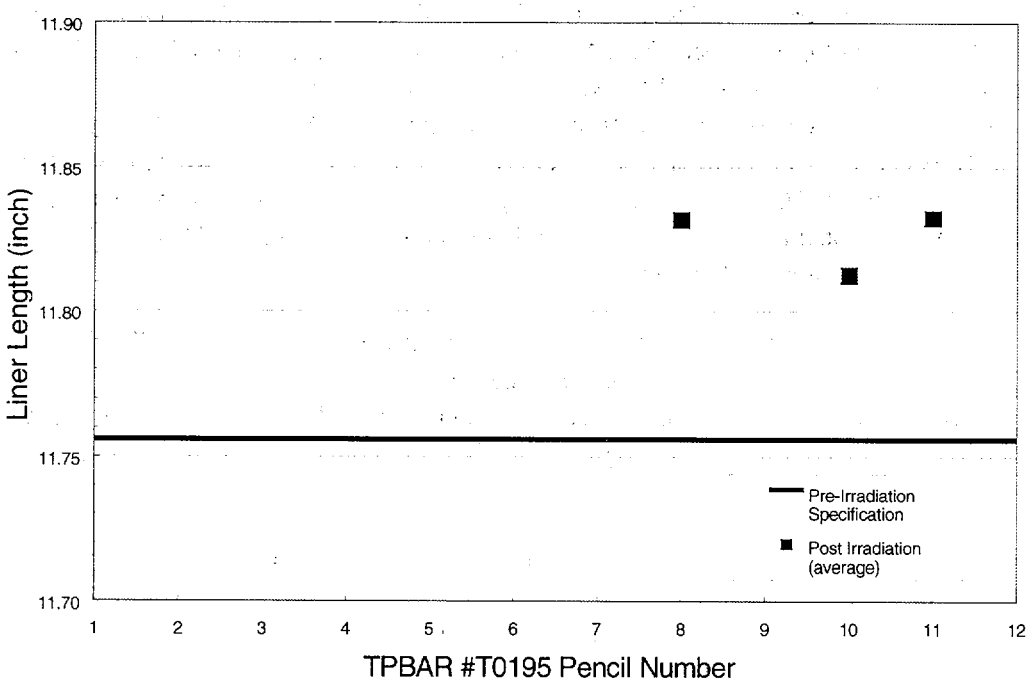


**Figure 20.** Comparison of Specified Pre-Irradiation Liner Length to Postirradiation Length Estimates for TPBAR T0195

# 3.0 Destructive Examinations

In this section, the TPBAR sectioning plans and the strategy for sampling/destructive analyses are summarized followed by general observations made during component separation. Selected assay results from the destructive quantitative analyses of the component samples are presented for each of the four TPBARs. Finally, evaluations of the resulting DE data are discussed.

## 3.1 TPBAR Segmenting for Shipment to PNNL

Because the full-length TPBARs (~153 inches long) were too long to be accommodated in PNNL's hot cells, ANL-W cut the four TPBARs that were to be sent to PNNL into three segments each. This cutting was done by ANL-W at locations on the TPBARs specified by PNNL. The resulting three segments for each TPBAR were a bottom segment consisting of the bottom end plug and pencils 1-4; a middle segment consisting of pencils 5-8; and a top segment consisting of pencils 9-12, the plenum region, and the upper end plug. The cutting was done by a milling operation; a through cut was assured when pellet powder was seen.

## 3.2 Summary of the Sectioning and Examination Plan

The four TPBARs selected for DE were T0166, T0195, T0281, and T0291. An analysis plan (Lanning 2000c) was developed for each TPBAR, consisting of a matrix of the radiochemical analyses required on the components from each TPBAR. It was decided to extensively examine only one TPBAR and then obtain confirmatory measurements from the other three TPBARs. TPBAR T0291 was selected for extensive DE because it had the higher predicted tritium production of the two TPBARs that were full-length gamma scanned (T0166 and T0291). The general strategy was to provide axial distribution for lithium burnup and component tritium, protium, and helium concentrations for TPBAR T0291 and to only spot-check these attributes on the other three TPBARs.

As specified in Lanning (2000c), sections were cut along the entire length of T0291, including the upper and lower end plugs, upper and lower getter disks, and pencil-pencil interfaces. For the confirmatory measurements, sections subsequently were cut from each end of the middle segments of the other three TPBARs. The top and bottom segments of TPBARs T0166 and T0195 were used for tritium extraction work.

To minimize the radiation dose for assay work, the sections were cut in 4-mm lengths. The individual components were then separated from the intact sections for the assays. For optical metallography and scanning electron microscopy, the sections were cut in 20-mm lengths to provide sufficient length for handling. The individual components were usually separated and then mounted individually to minimize problems associated with polishing dissimilar materials and to reduce the gamma dose of the mounted specimens during scanning electron microscopy.

Axial positions for sectioning to obtain samples were identified using the following considerations:

- Three adjacent sections in a midpellet location would provide a "standard suite" of examinations. These three sections would be used for 1) optical metallography and scanning electron microscopy (20 mm-long section); 2) tritium/protium assays of the getter and liner components and lithium isotopic assay of the pellet; and 3) tritium-only assays of the getter and liner components and tritium/He-4 assay of the pellet. A standard suite at the top and bottom of the middle segments of all four TPBARs was used to evaluate consistency for all TPBARs.

- Sections at pencil-pencil and pellet-pellet interfaces in T0291 would provide additional data.

- Getter end disks (upper and lower) plus sections of the plenum getter tube from both T0291 and T0281 would be analyzed for tritium and hydrogen.

- Sections capturing the upper and lower end plug weld regions on T0291 would be evaluated for integrity and indications of corrosion using optical metallography.

Examination locations were specified relative to the top of the TPBAR. The "top" was defined as the shoulder of the upper end plug. The sections of TPBARs were identified by the TPBAR number, the segment they were cut from (top [T], middle [M], or bottom[B]), and the sequential order. For example, section 281T-03 was the third section cut from the top segment of TPBAR T0281.

## 3.3 Rod Sectioning, Component Separation, and Data Analysis Approach

A special, automated, low-speed, diamond-wheel saw assembly was fabricated and commissioned in B-Cell of the High-Level Radiochemical Facility in the 325 Building at PNNL. The TPBARs were sectioned at low cutting speed (about 1 hour per transverse cut) and at nearly ambient temperature under argon gas. The cut sections were captured in metal tubes. The saw assembly permitted the positioning and sectioning of each TPBAR segment to an absolute accuracy of better than 1/8 inch relative to the end of the TPBAR segment.

As sample sections were sawed off, they were individually captured in pre-marked steel tubes, called "vials," with O-ring-sealed, press-fit end plugs. Cut sections remained in these vials until they were removed to separate the liner, pellet, and getter for examination. Observations and procedures for separation of the different types of sections are described below.

The liner generally fell out of the 4-mm sections and was recovered from the steel vial when it was opened. The pellet was easily punched out of the section (usually in one or two large pieces). The getter was harder to separate from the cladding, but could usually be punched out. Occasionally, the cladding would have to be "snipped" (cut with metal shears) to facilitate removal of the getter. An in-cell video camera was used to facilitate and document these activities and provide a photographic record of the appearance of the separated components.

The separated components were then placed in pre-marked, pre-weighed glass vials for transfer to the analytical laboratories. The glass vials were purged with argon and sealed. Air exposure of the component samples was limited to <1 hour. The vial tare weights were recorded to 0.1-mg accuracy, and the weights after sample insertion were taken to the same accuracy, to obtain milligram-level accuracy for the sample weights.

Notes on the actual sectioning results, results of component separation, and sections used for examinations are provided in Lanning (2000c).

The component assay procedures and data manipulating approaches are briefly described for each of the species assayed in the following sections. These descriptions include the manipulations by which reported data were processed to a form that can be compared to estimates of local linear production or TPBAR functional criteria; and example results are shown. For example, the results of tritium recovery from getter samples via high-temperature vacuum extraction are reported as tritium curies per gram of getter sample. This value is converted to curies per inch of getter, to compare to estimates of tritium production per inch of TPBAR.

### 3.3.1 Pellet Lithium Isotopic Analyses and Lithium Burnup Estimates

Entire, 4-mm-long, full-round pellet sections were crushed and homogenized prior to sampling for lithium isotopic distribution to obtain a representative pellet-average result. This action was taken to negate significant radial (through-wall) gradients in the pellet Li-6 burnup that are possible due to self-shielding effects within the pellet wall. Small aliquots of the crushed and mixed powder were prepared into acid slurries and loaded onto filaments. These filament samples were then vaporized and analyzed for lithium isotopic ratios by thermal ionization mass spectrometry. The Li-6 and Li-7 atom fractions in the material were measured from the results of nine separate runs on each sample, and spot-checked on duplicate slurry samples. The Li-6 burnup could only be derived by comparing these results to lithium isotopic fractions from unirradiated archive pellets. Therefore, archive LTA pellets were subjected to the same analysis procedure. The results for the archive pellets are also listed below.

The calculation of Li-6 burnup is as follows:

| | | |
|---|---|---|
| Xo, Zo | = | initial (unirradiated) atom fractions of Li-6 and Li-7, respectively |
| | | Xo = 21.30 atom % |
| | | Zo = 78.70 atom % |
| X, Z | = | measured (irradiated) atom fractions of Li-6 and Li-7, respectively |
| Ro | = | Xo/Zo = 0.27065 (unirradiated Li-6 to Li-7 ratio) |
| R | = | X/Z |

Because the number of Li-7 atoms remains constant, the Li-6 burnup, "B," (in % of initial Li-6 atoms) is given by:

B(%) = 100*(1 - R/Ro)

Thus, for example, the measurement of Li-6 burnup in a TPBAR section, with 11.8 atom % measured Li-6, is 100*(1.0 - 0.1338/0.27065) = 50.6%.

### 3.3.2 Tritium Recovery, Concentration, and Loading

The tritium concentrations were measured in pellet, getter, and liner samples. No cladding samples were analyzed for tritium or protium because 316SS cladding contains hardly any tritium or protium. The measurements were made by inductively heating the samples to melting temperature in a graphite crucible within a vacuum system, adding protium gas to provide isotopic swamping, then oxidizing the HT to THO, and condensing the tritiated water vapor in a cryogenic cold trap. The contents of the trap were then collected, diluted, and measured for tritium activity by liquid scintillation counting offline to determine the total tritium recovery. The scintillation counter was checked daily against a NIST standard.

The component samples were weighed before processing, and the tritium concentrations (curies per gram) were calculated by the total recovered tritium (in curies) divided by the sample weight. This concentration was reported together with the sample weight and the date of the counting. The conversion of this reported concentration to tritium recovery (Ci/inch) included a decay correction factor to correct the measured tritium activity to what it was at time-of-shutdown. Because of the 2.1 to 2.7 years between shutdown and counting, this correction factor ranged from 1.12 to 1.16, depending on the count date. The remainder of the conversion was different for each component, as described below.

#### 3.3.2.1 Pellet Recovery Calculation

From the pellet stack data reports, an average pellet mass per unit length was derived. This figure was multiplied by the reported concentration in curies per gram, and the decay correction applied to obtain the derived tritium concentration at shutdown in curies per inch.

#### 3.3.2.2 Liner Recovery and Loading Calculations

From the liner drawing and the liner stock material description, a Zircaloy mass per unit length was determined. This figure was multiplied by the reported concentration in curies per gram, and the decay correction applied to obtain the derived tritium concentration at shutdown in curies per inch.

#### 3.3.2.3 Getter Recovery and Loading Calculations

For the getters, the total mass/unit length (nickel + Zircaloy) was determined. The tritium concentration reported for the getters was tritium per gram of getter sample. To calculate the recovery, the reported concentration was multiplied by the total mass/unit length and the decay correction.

### 3.3.3 Protium Concentration and Loading

Protium was measured along with tritium in selected getter and liner samples by the following method. First, the sample was placed in a closed, evacuated volume and heated to a high temperature to drive off both protium and tritium. Next, the gas in this chamber was sampled and analyzed by mass spectrometry to determine the mole fractions of $T_2$, HT, and $H_2$ and, therefore, the H/T ratio. The

remaining gas was pumped through an analysis train consisting of a heated copper-oxide bed to oxidize the hydrogen isotopes to water vapor, and water bubblers to capture the tritiated water vapor. The contents of the bubblers were then scintillation-counted to obtain the absolute quantity of tritium that was evolved. A correction was made for the gas removed for off-line mass spectrometry, based on chamber/sampler pressure-volume-temperature measurements. The tritium was then reported as curies per gram of sample, and the protium was reported as H/T atom ratio, as calculated from the reported mass spectrometry results. To obtain the protium loading, the decay-corrected tritium loading was first calculated as outlined above. The protium loading (H/Zr) was calculated as the product of the tritium loading (T/Zr) and the reported H/T ratio, divided by the decay correction factor, since the H/T ratio involved decayed (as-found) tritium. Therefore, both tritium loading and protium loading data points were derived from a protium data report.

### 3.3.4 Pellet He-4 Recovery

The He-4 and tritium assays were conducted simultaneously for selected pellets. The pellets were placed in a graphite crucible in a chamber. The chamber was evacuated, and the pellets heated inductively to thermally evolve all gas from them. This gas was then spiked with a known quantity of He-3. The gas was sampled and analyzed for He-4/He-3 ratio by mass spectrometry. Correction was made for the He-3 (from postirradiation tritium decay) that was generated by the pellet, assuming all this decayed He-3 remained in the pellet. This procedure was corroborated by consistent retained-He-4 estimates with nearby unspiked samples, assuming all the He-3 in the unspiked samples was due to postirradiation tritium decay.

He-4 concentration was reported as STPcc/g of pellet. This was converted to helium recovery (STPcc/inch) by multiplying by the pellet average mass per unit length.

## 3.4 Assay Results for Individual TPBARs

This section provides the lithium isotopic results, lithium burnup, and pellet He-4 recovery for each of the TPBARs. Assay results for tritium recovery, tritium loading, protium loading, and hydrogen gettering rate were also determined, but these data are classified and are reported in Lanning et al. (2002).

### 3.4.1 Assay Results for T0291

A full axial distribution of assay measurements was obtained on TPBAR T0291 to provide a comprehensive picture of "performance" for one TPBAR.

The measured Li-6 and Li-7 concentrations and derived Li-6 burnup for samples taken from T0291 are presented in Table 7. Note that the measured Li-6 burnup ranges from 50% to 59%, which agrees with the predicted burnup of 50% to 60%.

The pellet He-4 data for T0291 are provided in Table 8.

**Table 7.** Lithium Isotopic Results and Lithium Burnup Estimates for T0291

| Section Number | Measured Li-6 in Total Li (atom %) | Measured Li-7 in Total Li (atom %) | Li-6/Li-7 Ratio | Calculated Li-6 Burnup (atom %) |
|---|---|---|---|---|
| Archive * | 21.30 | 78.70 | 0.27065 | -- |
| 291B-18 | 12.3 | 87.7 | 0.1403 | 48.2 |
| 291B-18 | 12.2 | 87.8 | 0.1390 | 48.7 |
| 291B-14 | 11.2 | 88.8 | 0.1261 | 53.4 |
| 291B-14 | 11.2 | 88.8 | 0.1261 | 53.4 |
| 291B-07 | 10.3 | 89.7 | 0.1148 | 57.6 |
| 291B-07 | 10.4 | 89.6 | 0.1161 | 57.1 |
| 291M-03 (Re-run) | 11.8 | 88.2 | 0.1338 | 50.6 |
| | 11.0 | 89.0 | 0.1236 | 54.3 |
| 291M-03 (Re-run) | 11.9 | 88.1 | 0.1351 | 50.1 |
| | 11.2 | 88.8 | 0.1259 | 53.5 |
| 291M-33 | 10.1 | 89.9 | 0.1123 | 58.5 |
| 291M-33 | 10.4 | 89.6 | 0.1161 | 57.1 |
| 291M-44 | 10.1 | 89.9 | 0.1123 | 58.5 |
| 291M-44 | 10.2 | 89.9 | 0.1135 | 58.1 |
| 291T-10 | 10.3 | 89.7 | 0.1148 | 57.6 |
| 291T-10 | 10.3 | 89.7 | 0.1148 | 57.6 |
| 291T-14 | 10.1 | 89.9 | 0.1123 | 58.5 |
| 291T-14 | 10.1 | 89.9 | 0.1123 | 58.5 |
| 291T-16 | 10.2 | 89.8 | 0.1136 | 58.0 |
| 291T-16 | 10.3 | 89.7 | 0.1148 | 57.6 |
| 291T-22 | 11.7 | 88.3 | 0.1325 | 51.0 |
| 291T-22 | 11.7 | 88.3 | 0.1325 | 51.0 |
| 291T-26 | 11.7 | 88.3 | 0.1325 | 51.0 |
| 291T-26 | 11.7 | 88.3 | 0.1325 | 51.0 |

* Average of seven measurements of unirradiated pellets from archive.

**Table 8.** He-4 Recovery Data on Pellets from TPBAR T0291

| Section Number | He-4 Recovery (STPcc/inch) |
|---|---|
| 291B-15 | 5.20 |
| 291B-06 | 5.43 |
| 291M-02 | 3.91 |
| 291M-32 | 4.56 |
| 291M-36* | 4.06 |
| 291M-45 | 6.75 |
| 291T-03 | 3.66 |
| 291T-13 | 5.69 |
| 291T-25 | 5.83 |
| 291T-29* | 6.11 |

* Indicates unspiked samples. All other results were evaluated from He-3-spiked gas samples.

### 3.4.2 Assay Results for T0281

Assay samples from TPBAR T0281 were taken primarily from the top and bottom of the middle segment (the chosen location for comparing assay results across all four TPBARs). A few getter and disk samples were also taken from the top and bottom of the TPBAR for tritium and protium assay.

The measured Li-6 and Li-7 concentrations and the derived Li-6 burnup for samples taken from T0281 are presented in Table 9. The measured Li-6 burnup for the middle segment of T0281 (~55%) agrees with the measured burnup for the middle segment of T0291 (50%-58%).

The pellet He-4 data for T0281 are presented in Table 10.

**Table 9.** Lithium Isotopic Results and Lithium Burnup Estimates for T0281

| Section Number | Measured Li-6 in Total Li (atom %) | Measured Li-7 in Total Li (atom %) | Li-6/Li-7 Ratio | Calculated Li-6 Burnup (atom %) |
|---|---|---|---|---|
| 281M-05 | 10.8 | 89.2 | 0.1211 | 55.3 |
| 281M-05 | 10.7 | 89.3 | 0.1198 | 55.7 |
| 281M-20 | 10.7 | 89.3 | 0.1198 | 55.7 |
| 281M-20 | 10.7 | 89.3 | 0.1198 | 55.7 |
| For archive isotopic results, see Table 7. | | | | |

**Table 10.** He-4 Recovery Data on Pellets from TPBAR T0281

| Section Number | He-4 Recovery (STPcc/inch) |
|---|---|
| 281M-04 | 4.31 |
| 281M-05 | 4.53 |

### 3.4.3 Assay Results for T0166

Assay samples from TPBAR T0166 were taken only from the top and bottom of the middle segment; the top and bottom segments were used for whole-segment extraction testing.

The measured Li-6 and Li-7 concentrations and derived Li-6 burnup for samples taken from T0166 are presented in Table 11. The measured Li-6 burnup for the middle segment of T0166 (~56%) agrees with the measured burnup for the middle segment of T0291 (50%-58%) and T0281 (~55%).

The pellet He-4 data for T0166 are presented in Table 12.

**Table 11.** Lithium Isotopic Results and Lithium Burnup Estimates for T0166

| Section Number | Measured Li-6 in Total Li (atom %) | Measured Li-7 in Total Li (atom %) | Li-6/Li-7 Ratio | Calculated Li-6 Burnup (atom %) |
|---|---|---|---|---|
| 166M-04 | 10.5 | 89.5 | 0.1173 | 56.7 |
| 166M-04 | 10.4 | 89.6 | 0.1161 | 57.1 |
| 166M-08 | 10.7 | 89.3 | 0.1198 | 55.7 |
| 166M-08 | 10.6 | 89.4 | 0.1186 | 56.2 |
| For archive isotopic results, see Table 7. | | | | |

**Table 12.** He-4 Recovery Data on Pellets from TPBAR T0166

| Section Number | He-4 Recovery (STPcc/inch) |
|---|---|
| 166M-03 | 4.39 |
| 166M-09 | 4.58 |

### 3.4.4 Assay Results for T0195

Assay samples from TPBAR T0195 also were taken only from the top and bottom of the middle segment, while the top and bottom segments were used for whole-segment extraction testing.

The measured Li-6 and Li-7 concentrations and derived Li-6 burnup for samples taken from T0195 are presented in Table 13. The measured Li-6 burnup for the middle segment of T0195 (~56%) agrees with the measured burnup for the other three TPBARs (50-58%).

The pellet He-4 data for T0195 are presented in Table 14.

**Table 13.** Lithium Isotopic Results and Lithium Burnup Estimates for T0195

| Section Number | Measured Li-6 in Total Li (atom %) | Measured Li-7 in Total Li (atom %) | Li-6/Li-7 Ratio | Calculated Li-6 Burnup (atom %) |
|---|---|---|---|---|
| 195M-04 | 10.6 | 89.4 | 0.1186 | 56.2 |
| 195M-04 | 10.6 | 89.4 | 0.1186 | 56.2 |
| 195M-08 | 10.9 | 89.1 | 0.1223 | 54.8 |
| 195M-08 | 10.9 | 89.1 | 0.1223 | 54.8 |
| For archive isotopic results, see Table 7. | | | | |

**Table 14.** He-4 Recovery Data on Pellets from TPBAR T0195

| Section Number | He-4 Recovery (STPcc/inch) |
|---|---|
| 195M-03 | 4.85 |
| 195M-10 | 4.32 |

## 3.5 Discussion of Li-6 Burnup Results

### 3.5.1 Total He-4 Production and Derived Li-6 Burnup

The tritium production and TPBAR-average lithium burnup (total atoms of Li-6 reacted) have been predicted with neutronics codes. The tritium production and TPBAR-average lithium burnup in the TPBARs have also been derived from the quantity of He-4 recovered on puncture (in excess of the 1-atmosphere fill gas during fabrication), modified by a correction for the residual He-4 in the pellets. This is because one atom of He-4 is produced in the lithium aluminate pellets for every atom of Li-6 reacted. See Table 6 for derived and predicted tritium production.

The method by which TPBAR total lithium burnup and total tritium/helium production were estimated is as follows:

1. Convert the pressure/void volume measurement results and the gas mass spectrometry analysis results from NDE rod puncture to moles of He-4 found in the end-of-life gas.

2. Subtract the quantity of He-4 initially present as fill gas.

3. Correct for measured residual He-4 left in the pellets.

The results of this calculation are shown graphically in comparison to the neutronics-calculated tritium production for all 32 TPBARs in Figure 17.

### 3.5.2 Li-6 Burnup from Isotopic Data Compared to Derived Burnup

Local measurements of Li-6 burnup, derived from measured pellet-average lithium isotopic ratios, are provided in Table 7, Table 9, Table 11, and Table 13.

For TPBAR T0291, the tritium production was 0.968 g and the TPBAR-average Li-6 burnup was given by the following:

0.968 g T / 3.016 g T/mole / (142 inch * 1.34 g pellet/inch / (6.8+27+32 g/mole pellet) * 0.2133 mole Li-6/mole Li) * 100%/fraction = 52.0%

The tritium production for TPBARs T0281, T0166, and T0195 were 0.918 g, 0.929 g, and 0.918 g, respectively, which corresponds to TPBAR-average Li-6 burnups of 49.4%, 49.7%, and 49.4% using the calculation described above.

The axial distribution of lithium burnup and, therefore, the axial distributions of tritium and helium production are estimated from the relative axial distribution of cladding activation, deduced from axial scans for Co-60 gamma activity reported in Lanning and Cunningham (2001).

To estimate the axial variation of Li-6 burnup, the Co-60 activity was least-squares curve-fit as a function of axial position. Then the curve-fit was normalized over the 142-inch pellet column portion such that the average value over that range equaled 1.0. This normalized curve equation is:

Normalized value = (0.326429 - 0.019951X + 0.00554X2 - 0.0002402X3 + 0.00000479538X4 - 0.0000000519044X5 + 0.000000000312455X6 - 0.0000000000009757X7 + 1.21378E - 15X8) * 1.036
where X is the distance from the top of the rod in inches.

This normalized curve was then multiplied by the 52.0% TPBAR-average burnup determined for TPBAR T0291.

For the other three TPBARs, the axial distribution found for TPBAR T0195 was assumed to apply. The normalized least-squares equation for this curve is:

Normalized value = (-1.031694 + 0.226917X - 0.010939X2 + 0.00030085X3 - 0.0000050966X4 + 0.00000005401017X5 - 0.000000000348456X6 + 0.0000000000012514X7 - 1.91945E - 15X8) * 1.019

This result was then multiplied by the 50.3% rod-average burnup for TPBAR T0195 and by the 49.7% rod-average burnup for TPBARs T0166 and T0281.

The axial distribution of Li-6 burnup for TPBAR T0291 is compared in Figure 21 to the measurements of Li-6 burnup derived from irradiated pellet lithium isotopic distributions. The two independent estimates of burnup distribution match within ~5% relative along the length of the TPBAR. This close agreement is confirmation of the calculated burnup axial distribution and, therefore, the tritium/helium production distribution for TPBAR T0291.

Similar comparisons between derived and measured Li-6 burnups are presented in Figure 22, Figure 23, and Figure 24 for TPBARs T0281, T0166, and T0195, respectively. The agreement is within 8% relative for each TPBAR, and this is confirmation of the tritium and helium production and distribution for these TPBARs.

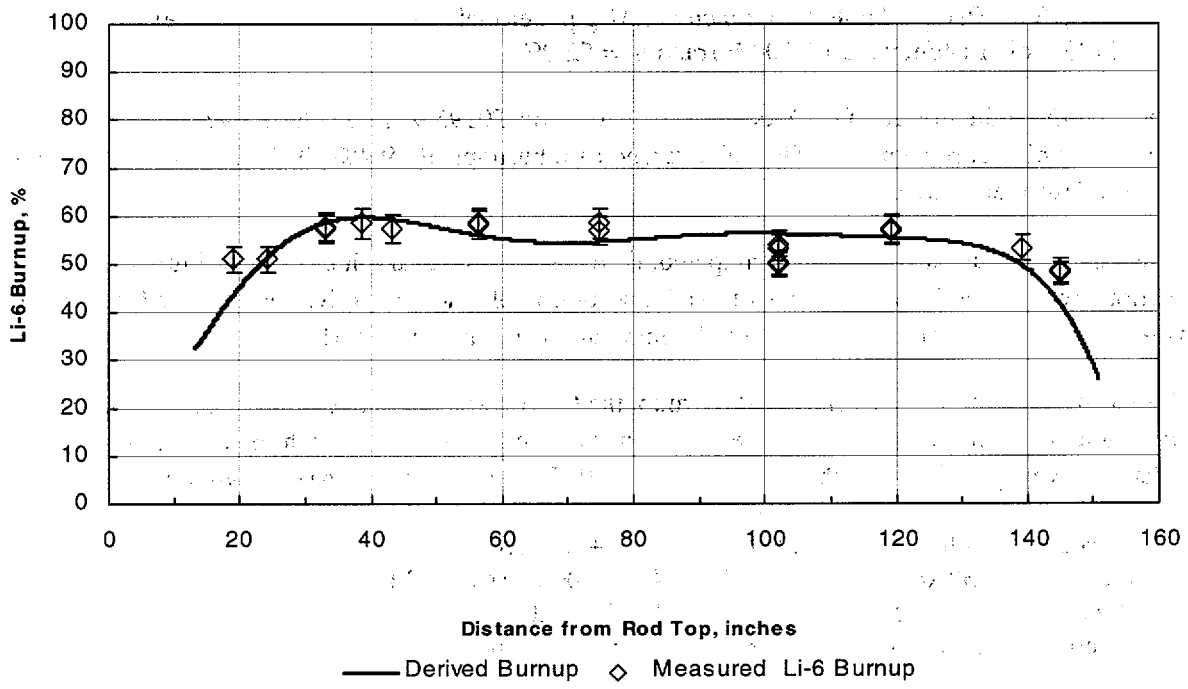


**Figure 21.** Measured and Derived Li-6 Burnup for TPBAR T0291

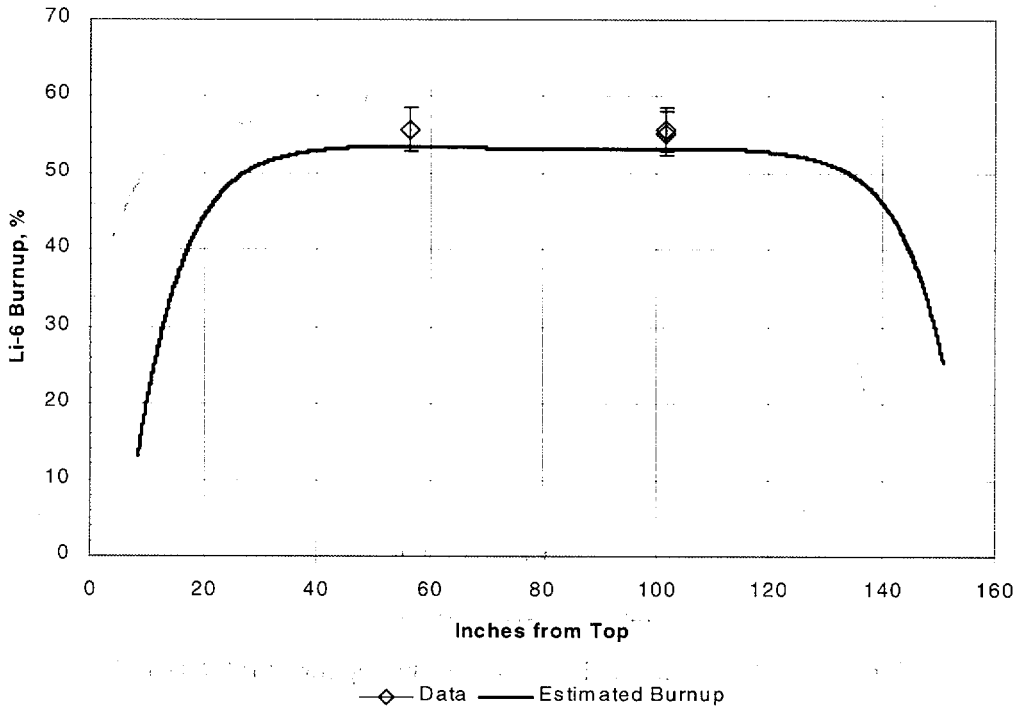


**Figure 22.** Measured and Derived Li-6 Burnup for TPBAR T0281

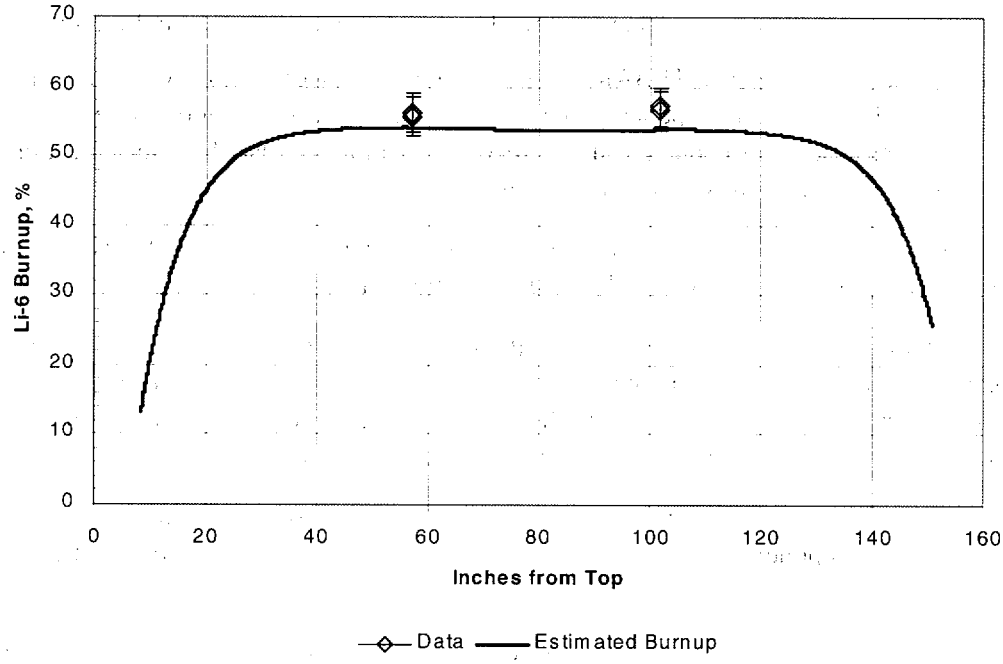


**Figure 23.** Measured and Derived Li-6 Burnup for TPBAR T0166

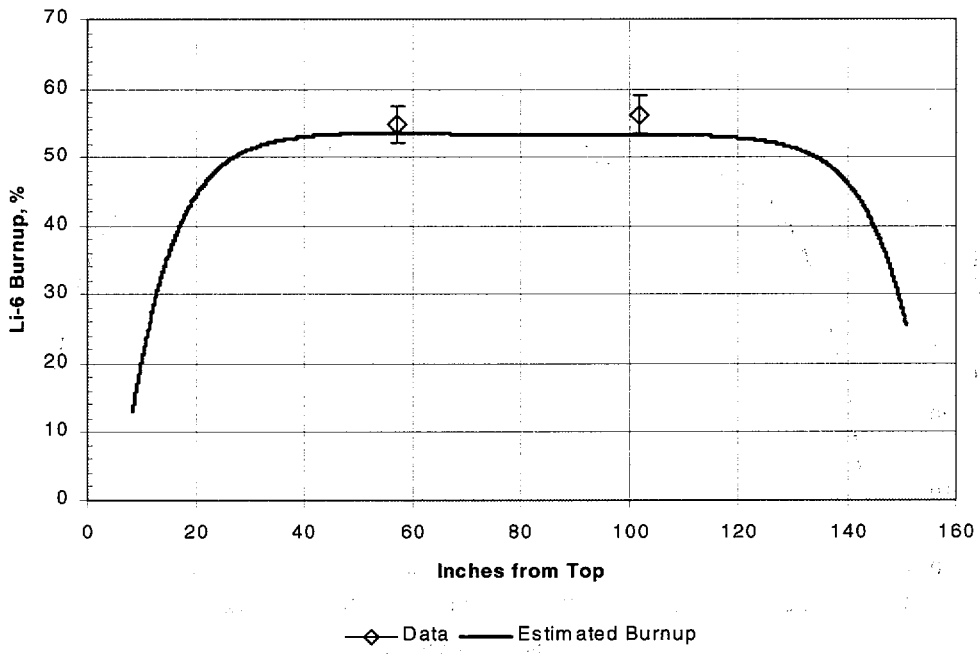


**Figure 24.** Measured and Derived Li-6 Burnup for TPBAR T0195

## 3.6 Evaluation of Tritium and Protium Assay and Getter Rate Results

Additional evaluations regarding tritium, protium, and getter rate results as described below were conducted. Details concerning these evaluations are classified and may be found in Lanning et al. (2002).

- At specified locations along each TPBAR, midpellet (non-interface) sections were taken for measurement of the tritium in the pellet, getter, and liner, and measurement of the retained He-4 in the pellet. The purpose was to obtain a sum of recovered tritium and He-4 at those locations, which could be compared to the locally generated values.
- The normalized burnup axial distribution curve was used to generate curves of linear tritium and helium production by renormalizing to the TPBAR-average linear production of each.
- The He-4 generated in the pellets at a given axial location was estimated in a manner similar to that for the generated tritium, by multiplying the TPBAR-average He-4 generation times the normalized generation distribution found from the fit to the Co-60 gamma activity. Then, the retained He-4 found in a pellet sample was compared to the locally generated value.
- To express the partition of tritium between getter, pellet, and liner on a consistent basis, the tritium recovery for each component in a non-interface section was divided by the estimated tritium production for that section.
- The getter protium data was used to infer the effective hydrogen ingress permeation reduction factor.
- Getter rate constants were measured for irradiated getter samples for comparison to nonirradiated samples and to the fabrication specification.

# 4.0 Optical Metallography

Samples examined by optical metallography were analyzed in a process similar to that used earlier to analyze irradiated ATR rod samples (Lanning et al. 1999). This work began in the High Level Radiation Facility (HLRF) hot cells at PNNL. Samples were then transferred to a mini-hot cell in the Shielded Analytical Laboratory for mounting, grinding, polishing, etching (as desired), and examination.

## 4.1 Sample Cutting

Samples were cut from the TPBAR segments using a sectioning saw in the HLRF hot cell. The samples supplied for metallographic examination were approximately 20 mm in length. The sectioning saw does not use a lubricant and damages the material as it cuts. Therefore, each sample was further sectioned using a slow-speed saw with a thin diamond-impregnated blade and using water as a lubricant and coolant. Each 20-mm section was cut in a manner that yielded samples approximately 7 mm long that were suitable for mounting. This also allowed sufficient material for archive purposes (to provide duplicates should a sample become damaged or react with the mounting media as was observed in the ATR examinations).

## 4.2 Sample Mounting

As the samples were cut, each component was separated and placed in individual, labeled sample vials. Each LTA component was mounted individually, rather than combined with other components as had been done for the ATR components. Many problems had been encountered with the ATR samples, including difficulty impregnating the samples with mounting resin and difficulty obtaining an optically flat surface due to the varying hardness of the components. Mounting the LTA samples individually helped to eliminate those problems.

All of the samples were mounted in a low viscosity, clear, epoxy resin. The resin was chosen for its sample adhesion and low shrinkage characteristics. The samples were potted under vacuum to remove bubbles. The best way to remove bubbles was to repeatedly apply vacuum, vent to atmosphere, and reapply the vacuum until most (if not all) of the bubbles were removed from the sample mounts. The samples were mounted in phenolic sample rings having a 32-mm diameter.

## 4.3 Sample Grinding

Planar grinding (rough leveling) and polishing of the samples was accomplished in the Shielded Analytical Laboratory mini-hot cell. Once the samples had been mounted, a small hole was drilled into the back of the samples to allow mounting on the polishers located in that hot cell. Diamond pads were used to perform the grinding on each sample. All samples were ground progressively from 30 μm (rough grinding) to 3 μm (fine grinding).

The samples were then subjected to progressive sanding steps using adhesive-backed silicon carbide sanding papers mounted to glass platens. Each sample was progressively finished starting at 120 grit and finishing at 1200 grit using deionized water as a coolant and lubricant. The samples were rinsed between each finishing stage with deionized water. Optical examination was performed at each step to ensure sanding scratches were uniform prior to moving to the next finer grit size. The optical examination was used to set the sanding operating parameters; the samples responded differently to the applied pressure and rotational speed of the sander. These settings are subjective and many hours were expended trying to get each sample as scratch-free as possible.

Following the finish sanding steps, the samples were polished. Adhesive-backed polishing cloths fixed to glass platens were used in the polishing operations. Water-based polycrystalline diamond slurries were purchased from several vendors for polishing. Polishing grit sizes ranged from 6 μm to 0.25 μm. Each sample was progressively polished from coarse to fine using clean, new polishing cloths at each step. Similar to the finish sanding steps, the polisher settings were selected as a function of the response of each sample to the polishing action.

Once polished, the samples were examined in the as-polished state, or etched and then examined.

## 4.4 Sample Etching

Most of the optical examinations were conducted on the samples in an as-polished state. However, often it was desirable to examine the microstructure further using etchants to reveal additional features. The etchants were selected for their ease of use, relative safety, and easy neutralization for waste disposal. A methanol-based aqua regia (56% HCl, 19% $HNO_3$, 25% methanol) was used to reveal the grain structure on iron-based components. A hydrogen fluoride-based etchant (<1% HF, 50% $H_2O_2$, 50% $HNO_3$) was used for zirconium alloys.

## 4.5 Optical Examination

An inverted Leitz metallograph fitted with a digitally controlled x-y-z motion stage and a digital black-and-white camera was used for the examinations. Stage motion control and image capture were computer controlled. A quartz-halogen light brought into the hot cell via a fiber-optic cable provided lighting. Images were stored digitally on the computer's hard drive or on compact disk. The images were printed from a personal computer equipped with graphics software and a high-resolution printer.

## 4.6 Examination Results

Detailed results from the examinations are provided in Lanning et al. (2002). Those results include the following observations:

- An end plug weld region was examined. The weld zone had a grain structure composed of laminar pearlite (as expected for a naturally cooled, untreated weldment). No corrosion was evident on the surface of the weld area, and the weld appeared to have no visible defects.

- The nickel plating on the getter appeared delaminated from the sample in places. This likely occurred during sample cutting and handling and was likely due to the polishing operation. The nickel plating conformed to the base material, which corroborates the concept that the delamination was due to the cutting and polishing operations.

- The microstructure of the pellets was uniform in nature, and the pellet did not appear to contain cracks, voids, or other defects.

- No signs of corrosion or other attack were noted on the exterior of the cladding that was exposed to the reactor coolant.

# 5.0 Conclusions

Thirty-two TPBARs were successfully irradiated during cycle 2 of the WBN plant and then nondestructively examined by ANL-W. Four of those TPBARs were then sent to PNNL for DE. Based on the data collected during the irradiation, the NDE of the 32 LTA TPBARs, and the DE of the four TPBARs, the following conclusions were reached:

- The TPBARs were intact following the irradiation, removal from the reactor core, and shipping to ANL-W. This was demonstrated by the following:
    - In-reactor performance of the TPBARs met the design limit of releasing less than 6.7 Ci of tritium per year per TPBAR.
    - The TPBARs had the expected helium atmosphere and pressure with no moisture when punctured.
- There were no difficulties in removing the LTAs from their host fuel assemblies and inserting them into the transportation arrays at the WBN plant, nor in then removing the TPBARs from the hold-down hardware at ANL-W.
- An adherent gray oxide covered all TPBARs and the hold-down hardware. Variations were seen in the oxide that likely resulted from flow variations in the guide tubes. Handling scratches were also seen in the oxide. Swipes of the TPBAR surfaces removed minimal amounts of material; the material removed was representative of typical reactor coolant system crud.
- Plenum gas pressure, void volume, and gas compositions were as expected upon TPBAR puncture. The measured tritium production ranged from 0.88 to 0.97 g tritium per TPBAR. The measured average tritium production was within 2% of the predicted average tritium production for the LTAs.
- Dimensionally, the TPBARs changed very little from their pre-irradiation condition. Postirradiation diameters were very near the fabrication specification of 0.381 inch. Postirradiation length was greater than the fabrication specification, but less than the bounding prediction for irradiation-induced growth. Rod bow was concluded to be minimal, at <0.5 inch over the TPBAR length.
- The neutron radiography revealed several internal features of the irradiated TPBARs. First, a large number of cracked pellets were observed; however, only negligible quantities of pellet were found outside of the pencils. Second, negligible gaps were observed between pencils. Finally, liners were observed to extend up through some pencil-pencil interfaces.
- Full-length axial gamma scanning confirmed the predicted tritium production profile. From these gamma scans, it was possible to detect pencil-pencil interfaces and fuel assembly spacer grid locations. In addition, there was minimal variation in gamma activity among TPBARs, thus confirming the expected minimal variation in neutron flux across the LTAs and host fuel assemblies.

The results of the tritium, hydrogen, helium, and lithium isotopic assays performed on samples obtained from the four TPBARs that were destructively examined confirm the in-reactor performance of the TPBARs determined from the nondestructive PIE data; that is, the TPBARs were successfully irradiated, produced the expected tritium quantities, and retained the tritium.

The overall conclusion from the NDE and DE of the LTA TPBARs is that the TPBARs remained intact throughout irradiation and postirradiation handling and shipping, and that the TPBAR components performed as designed. No indications were found of large dimensional changes or component physical or functional failures and no changes are required to the current TPBAR design.

# 6.0 References


Hagerty DM, and RO Gates. 1996. *TPBAR design drawings* (U). PNNL-TTQP-1-1024, Rev 0, Pacific Northwest National Laboratory, Richland, Washington.

Lanning DD, and ER Gilbert. 1998. *Information requirements for postirradiation testing of the LTA TPBARs* (U). PNNL-TTQP-1-686, Rev 0, Pacific Northwest National Laboratory, Richland, Washington.

Lanning DD, and ME Cunningham. 2001. *Evaluation report on nondestructive examination of LTA TPBARs* (U). PNNL-TTQP-3-528, Rev 0, Pacific Northwest National Laboratory, Richland, Washington.

Lanning DD, DL Baldwin, and SC Marschman. 1999. *Final report on postirradiation examination of Advanced Test Reactor test rods, Vol 1* (U). PNNL-TTQP-3-525, Rev 0, Pacific Northwest National Laboratory, Richland, Washington.

Lanning DD. 2000a. *Test plan for postirradiation examination of LTA TPBARs* (U). PNNL-TTQP-3-511, Rev 1, Pacific Northwest National Laboratory, Richland, Washington.

Lanning DD. 2000b. *Technical requirements document for the nondestructive examination of the LTA TPBARs by ANL-W* (U). PNNL-TTQP-3-509, Rev 2, Pacific Northwest National Laboratory, Richland, Washington.

Lanning DD. 2000c. *Sectioning and examination plan for the LTA TPBARs* (U). PNNL-TTQP-3-527, Rev 1, Pacific Northwest National Laboratory, Richland, Washington.

Lanning DD, DL Baldwin, ME Cunningham, and SC Marschman, 2002. *Results of nondestructive and destructive examinations on the LTA TPBARs* (U). PNNL-TTQP-3-542, Rev 0, Pacific Northwest National Laboratory, Richland, Washington.

McKee RS. 2000. *Measurements from the post-irradiation neutron radiographs of Watts Bar LTA TPBARs # T0166 & T0195* (U). PNNL-TTQP-1-763, Rev 0, Pacific Northwest National Laboratory, Richland, Washington.

Migliore RJ. 2000. PNNL-TTQP-3-517. *Watts Bar tritium data analysis for the lead test assembly* (U). Rev 0, Pacific Northwest National Laboratory, Richland, Washington.

Westinghouse. 1999. *Tritium production core (TPC) topical report (unclassified, non- proprietary version).* NDP-98-181, Rev 1, Westinghouse Electric Company, Monroeville, Pennsylvania.

# Distribution

| No. of Copies | OFFSITE |
|---|---|
| 10 | Office of Tritium Production, NA-125.1<br>U.S. Department of Energy<br>1000 Independence Avenue, SW<br>Washington, DC 20585 |

| No. of Copies | ONSITE | |
|---|---|---|
| 13 | Pacific Northwest National Laboratory | |
| | D. L. Baldwin | P7-22 |
| | M. E. Cunningham | K8-60 |
| | G. W. Hollenberg | K9-85 |
| | D. D. Lanning | K8-34 |
| | K. C. Larson | K9-85 |
| | S. C. Marschman | P7-27 |
| | B. D. Reid | K8-34 |
| | G. C. Sorensen | K9-85 |
| | C. K. Thornhill | K9-85 |
| | TTQP Records (2) | K9-85 |
| | Information Release (2) | K1-06 |